Beaulieu Jake, J (Orcid ID: 0000-0001-5750-0354)

Waldo Sarah (Orcid ID: 0000-0002-0185-1312)

Platz Michelle, C (Orcid ID: 0000-0002-3295-8112)

Methane and carbon dioxide emissions from reservoirs: controls and upscaling

Jake J Beaulieu[1*], Sarah Waldo[1], David A Balz[2], Will Barnett[3], Alexander Hall[1], Michelle C Platz[4], Karen M White[1]

[1]United States Environmental Protection Agency, Office of Research and Development, Cincinnati, OH 45268

[2]Pegasus Technical Services, Cincinnati, OH 45268

[3]Neptune Inc, Lakewood, CO 80215

[4]University of South Florida, Tampa, FL 33620

*Corresponding author: J.J.B. (email: beaulieu.jake@epa.gov)

Key Points

- Reservoirs are the fourth largest anthropogenic methane source in the US state of Ohio.
- Variables in national databases (reservoir size) predict methane emission rates nearly as well as variables measured on-site (nutrients).
- The global warming potential of methane emissions from reservoirs exceeded that of carbon dioxide emissions.

This article has been accepted for publication and undergone full peer review but has not been through the copyediting, typesetting, pagination and proofreading process which may lead to differences between this version and the Version of Record. Please cite this article as doi: 10.1029/2019JG005474

Abstract

Estimating carbon dioxide (CO_2) and methane (CH_4) emission rates from reservoirs is important for regional and national greenhouse gas inventories. A lack of methodologically consistent data sets for many parts of the world, including agriculturally intensive areas of the US, poses a major challenge to the development of models for predicting emission rates. In this study we used a systematic measurement approach to measure CO_2 and CH_4 diffusive and ebullitive emission rates from 32 reservoirs distributed across an agricultural to forested land-use gradient in the US. We found that all reservoirs were a source of CH_4 to the atmosphere, with ebullition being the dominant emission pathway in 75% of the systems. Ebullition was a negligible emission pathway for CO_2 and 65% of sampled reservoirs were a net CO_2 sink. Boosted regression trees (BRT), a type of machine learning algorithm, identified reservoir morphology and watershed agricultural land-use as important predictors of emission rates. We used the BRT to predict CH_4 emission rates for reservoirs in the U.S. state of Ohio and estimate they are the fourth largest anthropogenic CH_4 sources in the state. Our work demonstrates that CH_4 emission rates for reservoirs in our study region can be predicted from information in readily available national geodatabases. Expanded sampling campaigns could generate the data needed to train models for upscaling in other U.S. regions or nationally.

1 Introduction

Lakes and reservoirs are sites of intense carbon processing in the landscape. Carbon that enters lentic ecosystems through watershed runoff or internal primary production is subject to microbial transformations, often resulting in the production of the greenhouse gases (GHGs) carbon dioxide (CO_2) and methane (CH_4). It is estimated that lentic waters emit between 110 – 810 Tg CO_2-C y^{-1} (Cole et al. 2007, Tranvik et al. 2009, DelSontro et al. 2018) and 69-112 Tg CH_4-C y^{-1} (Bastviken et al. 2011, DelSontro et al. 2018) to the atmosphere each year, equivalent to roughly 20% of global CO_2 fossil fuel emission.

Emissions from reservoirs are of particular interest due to the complex tradeoffs between the societal services provided by reservoirs (i.e. hydropower, shipping, drinking water) and their environmental impact. Reservoirs have been recognized as sources of CO_2 and CH_4 since the early 90s (Rudd et al. 1993) and the World Bank, UNESCO, and International Hydropower Association encourage assessments of potential GHG emissions when planning dam infrastructure projects (International Hydropower Association 2010, Liden 2013, Prairie et al. 2017b). Furthermore, under the Intergovernmental Panel on Climate Change's (IPCC) GHG reporting framework, emissions from reservoirs are considered 'anthropogenic' and can be included in a nation's GHG inventory reported to the IPCC under the United Nations Framework Convention on Climate Change treaty, whereas emissions from lakes are considered 'natural' and therefore cannot be included in the GHG inventory. While the distinction between 'natural' and 'anthropogenic' emissions is an oversimplification, it has led to increased interest in quantifying GHG emissions from reservoirs. The recently adopted IPCC methodology (Lovelock et al. 2019) for estimating reservoir CO_2 and CH_4 emissions provides average emission rates (a.k.a. emission factors) for six major climate zones, but countries may choose to develop country specific emission factors or models, particularly where reservoirs constitute an important proportion of anthropogenic CH_4 and/or CO_2 emissions. Although earlier studies suggested that tropical reservoirs had higher CH_4 emission rates than temperate systems (Barros et al. 2011), a more recent data synthesis found little evidence for differences in emission rates among climate zones (Deemer et al. 2016), due partly to recent reports of high emission rates from eutrophic reservoirs in the United States and Switzerland (DelSontro et al. 2010, Beaulieu et al. 2014, Beaulieu et al. 2016, Beaulieu et al. 2018). Beaulieu et al. (2014) estimated that CH_4 emissions from reservoirs draining watersheds managed for corn and soybean production in the United States may emit 2.2 Tg CH_4-C y^{-1}, equivalent to 10% of the nation's annual anthropogenic CH_4 emissions. This estimate was derived by extrapolating measurements made at one agricultural reservoir to all US agricultural reservoirs and is therefore highly uncertain, but suggests that reservoirs may be an important component of the US anthropogenic CH_4 inventory.

Most attempts to upscale GHG emission rates from individual waterbodies to regional or global estimates simply multiply an average emission rate by the total waterbody surface area in the region of interest (St. Louis et al. 2000, Cole et al. 2007, Tranvik et al. 2009, Barros et al. 2011, Bastviken et al. 2011). This upscaling approach can be highly biased, however, unless the emission rate measurements come from a representative sample of lakes or reservoirs in the region of interest, which is unlikely. Most investigators choose sites based on convenience, the presence of research infrastructure, or other unique features. This set of criteria is unlikely to generate a collection of published emission rates that are representative of the population of lakes or reservoirs in the region. An alternative upscaling approach is to use published emission rate data to parameterize a statistical model relating emission rates to important drivers. Assuming the statistical relationships derived from the sample are applicable to the population, the model can be used to predict emission rates based on information about the population of lakes and reservoirs. In this approach, the sample data should come from waterbodies that cover a sufficiently large range of values for the explanatory variables, but do not need to be a representative sample of the population of interest. For example, Del Sontro et al. (2018) built statistical models relating CH_4, CO_2, and N_2O emission rates to measures of productivity (e.g. chlorophyll a, total phosphorus) and lake size. These models were then used to predict emission rates across the globe based on satellite derived measures of chlorophyll a and published lake size distributions.

Predicting emission rates from models is only possible if information about the model drivers is known at unsampled locations. Historically, this has been a major impediment to upscaling, but advances in remote sensing and geospatial modeling are beginning to address this. For example, the LakeCat database (Hill et al. 2018) contains 136 metrics describing watershed conditions (e.g. size, land use) for 378,088 waterbodies in the conterminous US and the LakeMorpho database (Hollister et al. 2011, Hollister and Stachelek 2017) contains information on morphometry (e.g. surface area, mean depth) for 363,314 waterbodies in the conterminous US.

Another limitation to upscaling reservoir GHG emissions in the US is a relative lack of published measurements. For example, total CH_4 emission rates (diffusive + ebullitive) for US reservoirs are only available for one reservoir in Ohio (Beaulieu et al. 2014, Beaulieu et al. 2016, Beaulieu et al. 2018), six reservoirs in the southeastern US (Bevelhimer et al. 2016), and six reservoirs in the pacific northwest (Harrison et al. 2017). Furthermore, the spatial and temporal resolution of the measurements vary among studies, complicating direct comparison of published rates.

The objectives of this work are to 1) identify important environmental drivers of CO_2 and CH_4 emission rates from reservoirs in the midwestern US, 2) upscale the measured emission rates to all reservoirs in one state in the region, and 3) test the model predictions against published emission rate measurements from other parts of the country. To achieve these objectives, we used a statistical survey design and consistent methodology to measure CH_4 and CO_2 emission rates from 32 reservoirs in Ohio, Kentucky, and Indiana. Emission rates were modeled using driver data collected from lakeCat, lakeMorpho, and on-site measurements (e.g. chlorophyll a, total phosphorus). We show that reservoir emission rates can be predicted from driver data contained in national databases and that there is little improvement in prediction accuracy when on-site measurements are included in the model. When upscaled to the U.S. state of Ohio, we found that reservoirs are the fourth largest anthropogenic CH_4 source. We also demonstrate that the model performs poorly when used to predict emission rates outside of the study region, suggesting that controls on reservoir GHG emission rates may vary by region.

2 Methods

2.1 Site selection and survey design

The survey was designed to include reservoirs that spanned a range of depth and watershed land-use conditions, two factors which can have a strong effect on CH_4 dynamics. Candidate sample sites included the Ohio reservoirs in the National Inventory of Dams (NID) (United States Army Corps of Engineers 2013) and the 21 reservoirs in the US Army Corps of Engineers (USACE) Louisville District. Reservoirs determined to be industrial waste ponds, offstream ponds, or part of a series of

reservoirs closely arrayed along a single river channel were omitted, leaving a total of 73 candidate reservoirs. Watershed land use was characterized for each candidate reservoir using 2011 NLCD data (U.S. Geological Survey 2014) and maximum reservoir depth was determined from bathymetric maps. Each reservoir was placed into one of sixteen groups representing the 16 unique combinations of four agricultural land use levels, based on the quartiles of the agricultural land-use distribution, and four maximum depth levels, also based on the quartiles of maximum depth distribution. Two reservoirs were selected from each of the 16 groups, resulting in 32 reservoirs distributed across Ohio, Kentucky, and Indiana (Fig. 1). This design resulted in a balanced compliment of shallow and deep reservoirs across the agriculture to forested land-use gradient in this three-state region. Each reservoir was sampled during a single contiguous two-day period between June 1 and September 14, 2016, except for Acton Lake which was also sampled on three dates in 2017 (Table S1). The sampling dates were chosen to reflect warm season conditions when waterbodies were stratified and CH_4 production rates were high.

A generalized random tessellation survey (GRTS) design (Olsen et al. 2012) was established for each of the 32 reservoirs using the spsurvey package (Kincaid and Olsen 2015) in R (R Development Core Team 2016). The GRTS design included a minimum of 15 sampling sites per reservoir, with up to 27 sites in the largest reservoir. To increase the accuracy and precision of the reservoir-scale emission rate estimates, areas immediately below the largest tributary inputs, where emission rates are often high and spatially variable (Beaulieu et al. 2014, Beaulieu et al. 2016), were sampled at a higher density than open-water portions of the reservoir. This stratification scheme was employed in 27 reservoirs with distinct 'tributary' and 'open-water' areas. Point estimates were scaled to population level estimates of mean and variance using an approach based on the Horvitz–Thompson theorem as described in Stevens and Olsen (2003) and implemented in spsurvey. Population level estimates from the four Acton Lake surveys were aggregated into a single estimate of mean and variance for the reservoir. Differences in emission rates among strata (open-water, tributary) within

individual waterbodies were assessed by comparing the 95% confidence interval of the estimate for each stratum.

2.2 Measurements

Ebullitive and diffusive CO_2 and CH_4 emission rates were measured at all sites. Water temperature, dissolved oxygen (DO), specific conductivity, pH, and chlorophyll a (chl a) were measured at a depth of 0.2 m below the water surface at all sites and 0.5 m above the sediment-water interface at the shallowest site. These parameters were also measured at 1 m depth intervals throughout the water column at the deepest site in each reservoir. Water samples were collected from 0.2 m depth for total nitrogen (TN), total phosphorus (TP), dissolved CH_4, and dissolved CO_2 at the deepest and shallowest sites. Barometric pressure was measured at the deepest and shallowest sites in each reservoir.

One reservoir from the survey, Acton Lake, was selected for additional measurements. An inverted funnel (described below) was deployed at a shallow (1.5m) and deep (12m) site at Acton Lake from May 15 – December 10 in 2016 and 2017. Gas was collected from the traps every two weeks and analyzed for CH_4 and N_2 content.

2.3 Emission rates

Short term floating chamber deployments were used to measure diffusive CO_2 and CH_4 emission rates (CO_2-D and CH_4-D, respectively). The dimensions of the aluminum chamber were identical to those of the CSIRO chamber presented in Zhao et al. (2015). The chamber floated on foam filled PVC pontoons with the chamber walls approximately 2.5 cm below the water surface. The headspace was mixed with a 0.658 m^3/min fan and vented through 0.48 cm i.d. x 12 m tubing to equilibrate the internal headspace pressure with the atmosphere. The tubing was sufficiently long to assure no gas exchange between the chamber headspace and atmosphere. The chamber headspace was interfaced to a DC operated gas analyzer (Ultra Portable Greenhouse Gas analyzer, Los Gatos Research, San Jose, CA, US) via 0.32 cm i.d. tubing. The analyzer continuously recirculated the chamber headspace during each 5 minute deployment and recorded H_2O, CH_4, and CO_2 partial

pressure every 5 seconds. A 10-point calibration curve was established at the beginning of the field season, verified at the end of the field season, and a one-point calibration check was performed in the field prior to each deployment.

Diffusive emission rates were calculated as

CH_4-D or CO_2-D = $(\Delta c/\Delta t)(V/A)(P/RT)$

where $\Delta c/\Delta t$ is the rate of change (ppmv h^{-1}) of CH_4 or CO_2 in the chamber headspace, V is the chamber volume (L), A is the area of the water surface enclosed by the chamber (m^2), P is the pressure (atm) inside the chamber (assumed to be equal to atmospheric pressure), R is the universal gas constant, and T is the air temperature (K). Diffusive emission rates were converted from mol m^{-2} d^{-1} to mg m^{-2} d^{-1} using the molecular weight of CO_2 or CH_4.

The CO_2 and CH_4 rate of change in the chamber headspace was quantified using a linear and non-linear model. The linear model assumes a constant emission rate during the deployment, whereas the non-linear model assumes a decreasing emission rate as the concentration gradient between the dissolved gas and the chamber headspace diminishes during the deployment (Stolk et al. 2009). The non-linear model is of the form

$c_t = c_{max} - [(c_{max} - c_0)\exp(-Kt)]$

where c_{max} (ppm) is the maximum concentration that can be reached in the chamber, c_0 (ppm) is the initial concentration, t is time, and K (min^{-1}) is a rate constant (Demello and Hines 1994, Stolk et al. 2009). The model was fit to the data using nonlinear least squares in the minpack.lm package (Elzhov et al. 2016) and the rate of change of CO_2 and CH_4 in the chamber headspace at t = 0 is calculated as

$\Delta c/\Delta t = K(c_{max} - c_0)$

The acceptance criteria for model fits was a coefficient of determination (r^2) of > 0.9 and the model best supported by the data was chosen using Akaike information criterion (AIC).

Ebullitive emission rates (CO_2-E or CH_4-E; mg m^{-2} h^{-1}) were measured using 0.56 m diameter inverted funnels suspended 0.8 m below an anchored buoy and topped with a gas collection reservoir

equipped with a ball valve and male luer lock fitting. Funnels were deployed between 10:00 and 21:00 (median deployment time = 14:44) and retrieved between 07:30 and 17:00 (median retrieval time = 10:28), for a median deployment duration of 19.4 hours (min = 14.5, max = 28.5 hours). Upon retrieval, the total volume of gas in the collection reservoir was measured using graduated polypropylene syringes and up to three 20 mL samples were transferred to pre-evacuated (<50 mTorr) 12 mL glass vials (Exetainers, LabCo, Wales, U.K.) equipped with a PTFE silicone septa stacked on top of a chlorobutyl rubber septa and analyzed for CH_4, CO_2, and N_2 partial pressure.

Ebullitive emission rates were calculated by multiplying the volumetric ebullition rate (mL m^{-2} h^{-1}) by the molar volume at the lake temperature (mol L^{-1}) and the fraction of CH_4 or CO_2 in the bubble gas. Finally, the molar ebullitive flux rate (mole m^{-2} h^{-1}) was converted to a mass flux (mg C m^{-2} h^{-1}). Total emission rates (CO_2-T or CH_4-T) were calculated as the sum of diffusion and ebullition.

To determine the net GHG footprint of the reservoirs, CH_4 emission rates were converted to CO_2-equivalents (CO_2-eq) using a 100-year time horizon Global Warming Potential (GWP) of 34 (Stocker et al. 2013). Due to their different lifetimes in the atmosphere, the warming potential of CH_4 relative to CO_2 depends on the timescale of interest and the IPCC provides different GWP values for 20, 100, and 500-year time horizons. Over time the C dynamics of flooded ecosystems tend to shift (Prairie et al. 2017a), calling into question the use of GWP for short-term studies (Frolking et al. 2006). We chose to use the 100-year time horizon for several reasons: 1) life-cycle analysis studies often assume a reservoir lifetime of 100 years (e.g., Gagnon et al. 2002, Prairie et al. 2017b), 2) to be consistent with the method used in the USEPA's National Inventory of Greenhouse Gas Sources and Sinks (US Environmental Protection Agency 2019b), and 3) to be consistent with many other published studies (e.g., Deemer et al. 2016, DelSontro et al. 2018).

2.4 Environmental variables

Duplicate dissolved gas samples were collected by pulling 115 mL of water into a 140 mL polypropylene syringe containing 25 mL of air and fitted with a 2-way stopcock. The stopcock was closed underwater, then the syringe was gently shaken for 5 minutes to equilibrate the gas and

water phases. Five mL of equilibrated headspace gas was used to flush the stopcock and attached 27 gage needle, and the remaining 20 mL transferred to a pre-evacuated (<50 mTorr) 12 mL glass vial (Exetainers, LabCo, Wales, U.K.). Triplicate 20 mL air samples were collected in 30 mL polypropylene syringes from 2.5 m above the water surface and transferred to pre-evacuated 12 mL glass vials. The dissolved CO_2 and CH_4 concentration in the original water sample was calculated from the Bunsen solubility coefficient at the temperature of the headspace equilibration, an assumed CO_2 and CH_4 partial pressure in the air (used as the headspace gas) of 405 and 1.85 ppm, respectively, and a mass-balance for the headspace equilibration system. Full documentation of the calculations is available at the National Ecological Observatory Network's GitHub repository (https://github.com/NEONScience/NEON-dissolved-gas).

Water temperature, DO, and chl a were measured using a YSI 6600 multiparameter sonde (Yellow Springs, Ohio, US) with an optical DO sensor and barometric pressure was measured using a YSI MDS 650. The data sonde was calibrated prior to each field day and the calibration was verified at the end of the day. Water samples for TP, TN, and TOC analysis were collected in new HDPE bottles triple rinsed with site water and stored on ice. Samples were stored at 5 ^{o}C and analyzed within 24 hours or frozen and analyzed within 28 days.

2.5 Analytical

Methane, CO_2, and N_2 were measured on a Bruker 450 gas chromatograph equipped with a flame ionization detector, methanizer, and thermal conductivity detector. Air, dissolved gas, and ebullition samples were analyzed in separate runs using a minimum of one 5-point standard curve bracketing the expected concentrations for each analyte. Standard curves were created using certified or primary standards, had a minimum r^2 of 0.990, and standard checks were analyzed throughout analytical runs.

Automated colorimetry (Lachat Instruments QuickChem 8000 Flow Injection Autoanalyzer, Loveland, CO, USA) was used to measure TP following acid persulfate digestion (Bogren 2001) and TN following alkaline persulfate digestion (Smith and Bogren 2003). TOC was measured using high temperature

oxidation and NDIR detection (Shimadzu TOC-L/ASI-L). Quality control measures included standard curves, standard checks, laboratory blanks, and matrix spikes.

2.6 Data analysis

2.6.1 Covariates

Potential predictor variables for modeling CO_2 and CH_4 emission rates include reservoir characteristics measured during the field campaign and those available in NHDPlusV2, lakeCat, and lakeMorpho, a group of related geo-spatial hydrologic data sets for the US (Hollister and Stachelek 2017, Hill et al. 2018, McKay et al. 2018).

Variables measured during the sampling campaign, hereafter 'local' variables, include measures of water chemistry (TN, TP, TOC, chl a, dissolved CO_2, dissolved CH_4) and relative volumes of the hypoxic layer (oxygen saturation < 5%) and hypolimnion. We defined the hypolimnion as the water layer below the plane with the greatest temperature gradient. Lakes where the temperature gradient did not exceed 1 C m^{-1} were considered unstratified.

NHDPlusV2, lakeCat, and lakeMorpho covariates, hereafter 'national' variables, include reservoir area, perimeter, max depth, mean depth, proportion littoral, climate data, and 128 variables describing watershed characteristics (i.e., land-use, size, soil properties). We recalculated the estimates of basin shape (i.e. depth) in NHDPlusV2, which were modeled based on the surrounding terrain (Hollister et al. 2011), using digitized bathymetric maps. We used the morphology descriptors included in the 'national' variables to calculate additional morphology descriptors. Shoreline development factor (D; Kalff 2002) was calculated as

$$D = \frac{L}{2(A\pi)^{0.5}}$$

where L is perimeter and A is area. Reservoir circularity (C), lake area relative to that of a perfect circle with circumference equal to L, was calculated as

$C = 4\pi AL^{-2}$

Dynamic ratio (DR; Hakanson 1982), an index related to the fraction of the lake bottom subject to erosion/resuspension from wind induced mixing, was calculated as

$$DR = \frac{A^{0.5}}{\bar{z}}$$

where $\bar{z}$ is mean depth calculated as the ratio of reservoir volume and surface area. The lakeMorpho dataset includes estimates of reservoir volume, but we recalculated volume using ArcGIS (ESRI, Redlands, CA, US) and the digitized bathymetry. Depth ratio was calculated as the ratio of mean to maximum depth (Kalff 2002) and the proportion of the lake < 3m deep, an index for littoral zone extent, was calculated using ArcGIS and the digitized bathymetry.

The list of potential predictor variables was reduced to those for which we hypothesized a relationship with CH_4 and/or CO_2 emissions. Correlation among predictor variables does not affect BRT prediction performance, but can confound model interpretation (Freeman et al. 2016, Fox et al. 2017). We therefore omitted one variable from any pair with a Pearson correlation coefficient > 0.9. Variable pairs that were more weakly correlated, but were likely to complicate model interpretation, were scrutinized, and in some cases, one variable in the correlated pair was dropped. For example, previous studies have shown that CH_4-D is negatively related to lake size (Rasilo et al. 2015) and positively related to shoreline development factor (Bevelhimer et al. 2016); however, these two variables were inversely correlated in our data set (R = 0.11), as has been reported in other studies (Winslow et al. 2014). This correlation could confound model interpretation; therefore shoreline development factor was omitted. The final list of predictor variables in the model consisted of 8 local and 12 national variables (Table 1).

2.6.2 Boosted regression trees

We modeled reservoir GHG emission rates using boosted regression tree (BRT) models, a type of machine learning (ML) algorithm. Given a sufficiently large training data set, ML algorithms have been shown to have better prediction accuracy than general linear models (glms) (Elith et al. 2008) and are increasingly used to model GHG emission rates in wetlands, lakes, and reservoirs (Papale and Valentini 2003, Mosher et al. 2015, Chen et al. 2018) .

Boosted regression trees consist of a collection of decision trees, where each tree is a statistical model that partitions the predictor space into regions that have the most homogenous values for a

response variable (Breiman et al. 1984, Elith et al. 2008). Typical tree-based methods generate a single tree, whereas BRT generates many trees using modern boosting algorithms (Schapire 2003) and combines them for prediction. This type of ensemble approach is based on the idea that individual trees often overfit the training data and result in noisy predictions. Averaging across many trees reduces the variance of the model and improves prediction accuracy.

We constructed separate BRT models for diffusive, ebullitive, and total CO_2 and CH_4 emission rates. Two types of models were constructed for each response variable; the first model type used only the 'national' covariates while the second model type used both the 'local' and 'national' covariates. This allowed us to asses 1) how well emission rates can be modeled using variables available for all waterbodies in NHDPlusV2, and 2) how much prediction accuracy improves when 'local' information is included in the model.

We constructed 50 BRT models for each response and covariate combination using the gbm package (Ridgeway 2017) in R. To minimize overfitting, each model was trained using 90% of the observations collected during this field study and tested against the remaining 10%. Cross-validation on the training data set was used to further minimize overfitting. To generate a training data set that reflected the full range of patterns across the 32 observations, the data were classified into 5 clusters, using K-means clustering, and the training data randomly selected from these 5 groups. A different training data set was generated for each BRT.

Each observation in the training data was weighted by the inverse of the variance of the reservoir-scale emission rate estimate. As described above (section 2.1), the variance was estimated from the GRTS survey design for each waterbody. This approach gave greater weight to well-constrained observations and less weight to more uncertain observations.

The optimal number of trees for each BRT was calculated as the number of trees beyond which model performance no longer improved. Only BRTs with an optimal number of trees > 1000 were accepted (Elith et al. 2008). Final BRT model performance was quantified as the mean square prediction error (MSE) calculated separately for the training data ("in-sample", or isMSE) and the

10% of the observations excluded from the training data ("out of sample", or osMSE). The collection of 50 BRTs for each response and covariate combination were ranked according to isMSE and osMSE. We defined the best model as the one with lowest sum of in and out of sample MSE rank, reflecting a balance between in and out of sample prediction error. Giving equal weight to in-sample and out-of-sample prediction error further minimized overfitting.

Standardized root mean square error (SRMSE) was calculated for all final models

$$\text{osSRMSE}=(\text{osMSE}^{0.5})\ (\text{mean response}^{-1})$$

$$\text{isSRMSE}=(\text{isMSE}^{0.5})\ (\text{mean response}^{-1})$$

where 'mean response' is the mean of the observed response variable in the training data. SRMSE is a measure of relative error and is therefore useful for comparing model performance across different response variables.

We use partial dependence plots, created with the pdp library (Greenwell 2017), to visualize relationships between response and predictor variables. Partial dependence plots provide a visualization of the relationship between the response and one predictor variable while accounting for the average effect of the other predictors in the model. The relative influence of predictor variables was calculated based on the number of times a variable is selected for splitting, weighted by the squared improvement to the model following each split, and scaled so that the sum of all variables adds to 100 (Elith et al. 2008).

2.6.3 Upscaling

We used the BRT to predict total CH_4 emission rates for a subset of waterbodies contained in the waterbodies layer of the NHDPlusV2 database for the US state of Ohio. The sample sites are distributed across the three main ecoregions in the state (Fig. 1), span a broad range of land-use conditions and reservoir morphometry, and are therefore representative of the environmental gradients most likely to affect emission rates. We adopted a state boundary to define our region of interest, rather than a more ecologically meaningful boundary, to facilitate comparison with emission sources in the FLIGHT database (https://ghgdata.epa.gov/ghgp/main.do) and

anthropogenic GHG inventory (US Environmental Protection Agency 2019b), both of which report emissions by state.

Reservoirs were identified from NHDPlusV2 Ohio waterbodies with FTYPE values of "LakePond" or "Reservoir" and surface area > 8 Ha. Smaller waterbodies (e.g. ponds) are given separate treatment in the IPCC methodology (Lovelock et al. 2019) and are not addressed here. Because the FTYPE codes in NHDPlusV2 are not reliable discriminating reservoirs from natural lakes (Clow et al. 2015), we used the following additional criteria to identify reservoirs: 1) an FTYPE value of 'reservoir' in NHDPlusV2, 2) GNIS name contained 'reservoir', 3) previous National Lakes Assessments (https://www.epa.gov/national-aquatic-resource-surveys/nla) site visits classified the waterbody as 'man-made', or 4) were located in close proximity to a dam in the National Inventory of Dams (NID) database (United States Army Corps of Engineers 2013). Finally, the identified waterbodies were merged with the lakeCat and lakeMorpho databases to capture catchment and morphology descriptors.

To upscale to an annual estimate, we assumed 1) our measured rates were representative of April – October conditions (7 months), and 2) emission rates declined to a low and constant rate of 1 mg CH_4 m^{-2} h^{-1} from November through March (Beaulieu et al. 2014; https://ameriflux.lbl.gov/sites/siteinfo/US-Act, Beaulieu et al. 2018). We calculated 95% confidence intervals for the upscaled emission estimate by repeating the calculations 1000 times where each calculation was based on a bootstrapped sample (with replacement) of the reservoirs in Ohio (Efron 1979). This non-parametric manner of estimating uncertainty is well-accepted in the statistical literature and allows the modeler to simulate replication by sub-sampling the data set a large number of times.

3 Results

3.1 Basic site description

The survey design resulted in a collection of reservoirs spanning a broad range of morphological and chemical conditions. Sampled reservoirs ranged from 1 – 32 km^2 in surface area (median = 4.6 km^2)

with maximum depths ranging from 2.7 – 35 m (median = 11.0 m) (Table 1). Watershed land use across the 32 reservoirs was predominantly cultivated lands in the western portion of the study area transitioning into forested lands in the east and south (Fig. 1). This broad range of watershed condition was reflected in the water chemistry with TP, TN, and chla ranging from 7.9 – 773, 231 – 3463, and 1.5 – 61.4 μg L^{-1} across the study sites, respectively, and exhibiting positive correlation with percent cultivated land in the watershed (R = 0.36, 0.78, and 0.50, respectively). Twenty-four reservoirs were thermally stratified at the deepest sampling site and 22 reservoirs had hypoxic bottom waters.

3.2 Emission rates

Dissolved CH_4 was supersaturated at all sites (Table 1, range 0.43 – 18.55 μmol L^{-1}, median = 2.95 μmol L^{-1}), indicating that all reservoirs were a source of CH_4 to the atmosphere. This was reflected in CH_4-D which ranged from 0.03 – 21.99 mg CH_4 m^{-2} h^{-1} across the 491 individual measurements that met the modeling acceptance criteria (see Methods). When aggregated to the reservoir-scale, CH_4-D ranged from 0.11 – 4.95 mg CH_4 m^{-2} h^{-1} (Fig. 2; median = 1.26 mg CH_4 m^{-2} h^{-1}). Methane ebullition rates ranged from 0 to 155.4 mg CH_4 m^{-2} h^{-1} (Fig. 2; median = 0.96 mg CH_4 m^{-2} h^{-1}) across 536 individual measurements and averaged 5.0 mg CH_4 m^{-2} h^{-1} at the reservoir scale (range: 0.1 – 22.8 mg CH_4 m^{-2} h^{-1}). Bubble CH_4 content ranged from 0.01 – 86.3% CH_4 (median = 57.4%, n = 336) and was inversely related to bubble N_2 content (Fig. 3A). Total CH_4 emission rates (diffusive + ebullitive) ranged from 0.03 – 155.4 mg CH_4 m^{-2} h^{-1} across all point measurements and averaged 1.47 mg CH_4 m^{-2} h^{-1} when aggregated to the whole-reservoir scale (Fig. 2; range: 0.51 – 24.57 mg CH_4 m^{-2} h^{-1}). Total CH_4 emission rates ranged from 5.1 – 12.3 mg CH_4 m^{-2} h^{-1} across the four surveys at Acton Lake (Table 2) with an overall mean (+/- 95% CI) of 9.2 +/- 3.0. The total CH_4 emission rate was greater in the tributary than open-water strata in 21 of the 27 reservoirs where a stratified survey design was used, although the difference was statistically significant in only 8. On average, ebullition composed 65% of total CH_4 emissions (range: 11 – 99%) with diffusive emissions accounting for the balance.

Dissolved CO_2 ranged from 26.0 – 244.9 µmol L^{-1} (Table 1, median = 113.5 µmol L^{-1}), equivalent to 28 – 278 % of the saturation value. Reservoir scale CO_2-D ranged from -92.8 – 193.1 mg CO_2 m^{-2} h^{-1} (median = -41.0 mg CO_2 m^{-2} h^{-1}). Trapped bubbles contained minor amounts of CO_2 (range: 0.02 – 8.8%, median = 0.19%) and CO_2 ebullition constituted only 0.63% of total CO_2 emissions, on average. Reservoir-scale CO_2-T ranged from -93 - 193 mg CO_2 m^{-2} h^{-1} (Fig. 2, median = -40 mg CO_2 m^{-2} h^{-1}) and 21 reservoirs exhibited net CO_2 uptake during the measurement campaign (Fig. 2D).

Although all 32 reservoirs were CH_4 sources during the survey, the GWP of these emissions was completely offset by CO_2 uptake in 11 reservoirs, yielding a net negative GWP for combined CH_4/CO_2 emissions using the 100-year time horizon (Fig. 2E). The remaining 21 reservoirs yielded a positive net GWP of CO_2/CH_4 emissions, despite 10 of them functioning as CO_2 sinks. If the 20-year GWP was used to compare CH_4 to CO2, all reservoirs would have had larger and more positive combined GWP.

3.3 Boosted regression trees

Boosted regression trees for diffusive, ebullitive, and total CH_4 emission rates fit the data well with isSRMSE values ranging from 0.11 – 0.40 and R^2 values for predicted vs observed (in-sample) ranging from 0.87 – 0.99 (Table 3, Fig. S1). Model predictions were less accurate at high emission rates, likely because these observations had larger confidence intervals (Fig. 2) and were therefore given less weight in the model. As expected, model performance was somewhat greater when assessed against the training data than testing data. On average, osSRMSE values for the CH_4 models were 78% greater than isSRMSE values. Model performance was best for the total CH_4 emission rate, followed by ebullitive and diffusive emission rates. Combining local covariates (i.e. nutrient chemistry) with national covariates (i.e. watershed land use) improved CH_4 model performance when assessed against the training data, but not when assessed against the testing data.

Indicators of watershed agricultural land use were important predictors in all CH_4 models and descriptors of reservoir morphology were important predictors in most CH_4 models (Table 3, Fig. 4). Reservoir area predicted diffusive CH_4 emissions and max depth predicted ebullitive and total CH_4 emissions. The BRT that included local covariates for CH_4-D identified TOC, dissolved CH_4, and TP as

important predictors. Proportion hypolimnetic and dissolved CO_2 were important local predictors for CH_4-E and CH_4-T.

Prediction accuracy of the CO_2-T BRT was worse than that of the CH_4 models (Table 2). The CO_2-T model informed by only national covariates identified littoral extent and agricultural on steep slopes as important predictors. The addition of local covariates, particularly dissolved CO_2, improved model performance.

3.4 Upscaling

We identified 280 reservoirs in Ohio greater than 8 Ha. These reservoirs have a cumulative surface area of 479 km^2 and emit 21.3 (13.3 – 30.8) Gg of CH_4 per year.

4 Discussion

4.1 CH_4 emission rates

CH_4-T estimates for the individual reservoirs included in this study are reasonably well constrained and compare well to the literature. Total CH_4 emission rates measured in our diverse collection of 32 reservoirs spanned an order of magnitude (0.51 – 24.57 mg CH_4 m^{-2} h^{-1}), with higher rates occurring predominantly in the agricultural plains in the northwestern portion of the study region and lower rates in the Appalachian foothills of the eastern and southern portions of the study region (Fig 2). These emission rates are within the range reported for reservoirs worldwide (Deemer et al. 2016) and are comparable to values reported for other reservoirs in this region. In an investigation of six large, forested reservoirs in the southeastern US, Bevelhimer et al. (2016) reported reservoir-scale CH_4-T ranging from 0.04 – 1.07 mg CH_4 m^{-2} h^{-1}, similar to our values for forested reservoirs in the eastern and southern portions or our study (i.e. PDT, CFK). Beaulieu et al. (2018) monitored CH_4-T at William H. Harsha Lake, an agricultural reservoir in southwestern Ohio that was also included in this study (EFR), and reported an average CH_4-T of 34.3 mg CH_4 m^{-2} h^{-1} between April and December 2015, which is similar to the highest rate observed during this study (mean +/- 95% CI: 24.6 +/- 7.59 mg CH_4 m^{-2} h^{-1}), but higher than the current Harsha Lake measurement (mean +/ 95% CI: 10.1 +/- 5.2 mg CH_4 m^{-2} h^{-1}), likely due to daily/seasonal variation in emission rates (section 4.2) and/or

differences in measurement methods between sampling campaigns (Beaulieu et al. 2018). Although there are few published studies of CH_4 emission rates from reservoirs in this region of the US, the available data suggest a pattern of increasing emission rates across an agricultural to forested land-use gradient.

Because CH_4 is a relatively insoluble gas, it is often emitted in the form of bubbles that are released from the sediment and rise through the water column. Ebullition was an important emission mechanism in this study, comprising >50% of total CH_4 emissions in 75% of the 32 sampled reservoirs (Fig. 2). This compares well to reports that ebullition contributes 65% of total CH_4 emissions from individual reservoirs (Deemer et al. 2016) and between 40-60% of total emissions from individual natural lakes (Bastviken et al. 2004). Comparison of CH_4-E among lakes and studies can be complicated, however, by differences in bubble composition. The CH_4 content of bubbles collected in this study ranged from 0.01 – 86.3% CH_4 (median = 57.4%), similar to the range previously reported for lakes (Walter et al. 2008) and reservoirs (Harrison et al. 2017, Koschorreck et al. 2017, Beaulieu et al. 2018). Bubble CH_4 content was inversely related to N_2 content (Fig. 3A), a pattern which has also been observed in lakes and wetlands (Chanton et al. 1989, Nakagawa et al. 2002, Walter et al. 2008) and is attributed to N_2 stripping. N_2 stripping occurs when ebullition removes N_2 from porewaters more quickly than it is replenished via diffusion from the overlying water column, thereby depleting sediment N_2 content and enriching the CH_4 content of rising bubbles (Chanton et al. 1989). Stripping likely contributed to the increasing bubble CH_4 content from June through October observed at Acton reservoir (ACT; Fig.3B). Falling bubble CH_4 content in November and December likely reflects decreasing volumetric ebullition rates as the water column cooled, allowing diffusion to replenish porewater N_2. Patterns in porewater N_2 stripping, in combination with temporal changes in temperature, organic matter availability, and other factors, can lead to complex spatial and temporal patterns in CH_4 ebullition.

4.2 Survey and measurement approach

Although it is becoming increasingly evident that ebullition is an important CH_4 emission mechanism in lentic waters, it remains challenging to quantify due to strong spatial and temporal variability. In this study, we characterized spatial variability within the framework of a generalized random tessellation survey (GRTS) design (see section 2.1). Features of the GRTS design that make it particularly well suited for estimating CH_4-E and CH_4-T include 1) a spatially balanced distribution of sampling sites (Olsen et al. 2012), thereby better representing the full range of environmental conditions present within a waterbody as compared to random sampling, and 2) the ability to utilize spatial autocorrelation to better constrain variance estimates. In this study, variance estimates were reduced by 23% when spatial autocorrelation was incorporated into the estimate, indicating strong spatial autocorrelation in CH_4-T, as has been reported elsewhere (Beaulieu et al. 2016, Hilgert et al. 2019). The median 95% confidence intervals for CH_4-T and CO_2-T were 72.3 and 58.2% of the mean emission rate, respectively. Given that the observed CH_4 emission rates spanned two orders of magnitude in this study, an uncertainty estimate equivalent to ~ 70% of the mean is acceptable for the purposes of training a model for predicting emissions at unsampled locations. Furthermore, our modeling approach used the uncertainty estimate to give more weight to well constrained estimates, thereby ensuring that model results weren't driven by highly uncertain observations. We suggest that studies of lentic CH_4 and CO_2 emission rates be based on robust survey designs that form the basis for well-defined variance estimates.

Sampling tributary-associated areas at a higher density than open-water areas allowed for a better constrained and more accurate population estimate than if the entire waterbody had been sampled at a uniform density. Other studies have attributed tributary associated CH_4 hots spots to higher temperatures at the sediment-water interface, high sediment deposition rates, and sustained nutrient inputs from inflowing rivers which support phytoplankton, a source of particularly labile carbon for methanogens (DelSontro et al. 2011, Grinham et al. 2011, Musenze et al. 2014, Sturm et al. 2014, de Mello et al. 2018, Hilgert et al. 2019). Low water depths in tributary areas minimizes the

dissolution of bubbles during vertical transport through the water column, further enhancing CH4 emissions (McGinnis et al. 2006). Our finding that tributaries supported higher CH_4-T than open-waters in 21 of the 27 reservoirs where stratification was employed (although the difference was only statistically significant in 8) further highlights the importance of including tributary areas in reservoir-scale emission estimates.

Methane emission rates can exhibit temporal variation at time-scales ranging from hourly to yearly (Natchimuthu et al. 2016, Harrison et al. 2017, Maher et al. 2019). Our survey was designed to represent a snapshot of conditions during the growing season. Ebullition, the most important emission mechanism in most of the sampled reservoirs, was measured throughout ~19 hour (median = 19.4 hour) funnel deployments, encompassing roughly equal hours of daylight and dark. Our ebullition rate estimates should therefore integrate across diurnal patterns and reflect emission rates similar to 24 hour daily integrated vales. Diffusive emissions were measured during a short 5-minute window of daylight, however, and could be biased if a diurnal pattern were present. While several studies have documented diurnal patterns in CH_4-E (Deshmukh et al. 2014, Maher et al. 2019), the literature on diurnal patterns in CH_4-D is somewhat mixed. For example, Carey et al. (2017) failed to find a consistent diurnal pattern in CH_4-D in a productive US reservoir. Natchimuthu et al. (2014) reported higher dissolved CH_4 concentrations during daylight hours in a small pond (average depth = 1.2m), but it isn't clear how patterns from a shallow pond would translate to patterns in our much larger reservoirs. Recent eddy-covariance studies have shown evidence of diurnal patterns in CH_4 emission rates, but the results are mixed and it is difficult to distinguish ebullition and diffusion using this method (Podgrajsek et al. 2014, Erkkila et al. 2018) Given the conflicting and sparse literature data, it is difficult to know whether the short-term CH_4-D measurements in this study are biased. Bias in CH_4-D would not greatly affect the total emission rate estimate when ebullition was the dominant emission mechanism (Fig. 2), as was the case in 75% of the sampled reservoirs, but would be a concern where CH_4-D and CH_4-T were similar.

The four surveys conducted at Acton Lake indicate that CH4-T can vary by up to a factor of 2.4 within the warm weather months (Table 2; range : 5.1 - 12.3 mg CH_4 m^{-2} h^{-1}). This variation could be caused by numerous factors including changes in hydrostatic pressure, which can trigger the release of bubbles stored in sediments (Varadharajan and Hemond 2012, Harrison et al. 2017), availability of algal derived carbon (West et al. 2016), or extent of porewater N_2 stripping (section 4.1). While the temporal variability observed at Acton Lake was substantial, it was less than the variation observed across the 32 study sites (Fig. 2; range: 0.51 – 24.57 mg CH_4 m^{-2} h^{-1}) or within Acton Lake during any of the four surveys (within lake CH_4-T maximum exceeded minimum by a factor of 43, on average, data not shown), suggesting that that spatial variability (both intra and inter reservoir) exceeds temporal variability. Nevertheless, temporal variability may introduce uncertainty and bias into model predictions. Sampling on randomly selected days, as was done in this study, is likely to miss episodic emission events, which appear to be responsible for most day to day variability in CH_4-T (Varadharajan and Hemond 2012), resulting in emission rate estimates that are biased low (Wik et al. 2016). Quantifying model uncertainty resulting from temporal variability is challenging, but emerging continuous monitoring approaches may allow for this in future studies (Jammet et al. 2017).

4.3 CO_2 emission rates

Ebullitive CO_2 emissions were negligible compared to diffusive emissions in most reservoirs. This pattern is expected because CO_2 is a relatively soluble gas with most produced CO_2 dissolving into the water column or pore waters, rather than accumulating in bubbles. Our findings are consistent with reports that CO_2-E is less than 0.05% that of CO_2-D in large reservoirs in the Southeastern US and Brazil (Bergier et al. 2011, Kemenes et al. 2011, Bevelhimer et al. 2016), suggesting this pattern is common across a broad range of lentic ecosystems.

Reservoir-scale CO_2 emission rates were highly variable across the 32 reservoirs (-93 - 193 mg CO_2 m^{-2} h^{-1}), spanning nearly the entire range of reservoir CO_2 emission rates found in the published literature (-54.4 - 403 mg CO2 m^{-2} h^{-1}; Deemer et al. 2016), reflecting the broad range of watershed

and reservoir conditions in this study. Sixty five percent of the reservoirs functioned as CO_2 sinks during the sampling period, which contradicts findings from several global-scale and regional-scale studies. In a study of 1835 lakes with a worldwide distribution, Cole et al. (1994) reported that only 13% were CO_2 sinks. Similarly, Deemer et al. (2016) found that only 16% of published studies report net CO_2 uptake in reservoirs and studies in boreal regions routinely report net CO_2 efflux (Sobek et al. 2003). Reports of CO_2 emission rates for US lakes and reservoirs are more mixed, however. A national-scale survey of dissolved CO_2 found 35% of sampled US waterbodies (n = 1080) to be CO_2 sinks with no coherent spatial pattern (Lapierre et al. 2017), whereas regional studies suggest strong geographic variation. For example, measurements in the southeastern US indicate net CO_2 evasion from >85% of sampled lakes and reservoirs (n = 954) (Lazzarino et al. 2009, Bevelhimer et al. 2016), whereas surveys of lakes and reservoirs in the western and midwestern US indicate a predominance of CO_2 uptake (Soumis et al. 2004, Balmer and Downing 2011) during the summer months, particularly in systems draining agricultural watersheds. These contrasting results for US waterbodies highlight the difficulty in predicting lentic CO_2 emission rates. This is also reflected in the poor prediction accuracy of the CO_2-T BRT model developed in this work, relative to that of the CH_4-T BRT. One possible explanation for this is that the controls on CO_2 emissions may vary across the major US ecoregions. For example, Lapierre et al. (2017) found geographically varying driver-response relationship for dissolved CO_2 in US waterbodies reflecting major landscape gradients across the country. The 32 reservoirs included in our study span three major ecoregions (Fig. 1), roughly corresponding to regions identified by Lapierre et al. (2017) to have different dissolved CO_2 ~ driver relationships, suggesting that spatially explicit modeling approaches may improve prediction accuracy for lentic CO_2 emission rates.

Like many other studies of air-water CO_2 exchange in lentic ecosystems, we measured diffusive CO_2 emission rates during daylight hours. While these short-term measures of CO_2-D have been used to inform global CO_2 budgets for lentic systems (Cole et al. 2007, DelSontro et al. 2018), they may not reflect a daily integrated rate. Diurnal changes in the relative rates of CO_2 uptake (photosynthesis)

and production (respiration) can be pronounced, particularly in productive waterbodies, leading to higher emission rates during hours of darkness. This pattern has been reported for a wide range of lentic ecosystems including lakes in northern Europe, Canada, Brazil, and China (Vesala et al. 2006, Natchimuthu et al. 2014, Reis and Barbosa 2014, Du et al. 2018, Erkkila et al. 2018, Spafford and Risk 2018). Perhaps more relevant to the current study are reports from a eutrophic lake and reservoir in the southcentral US (Liu et al. 2016, Xu et al. 2019). During the summer months, both systems alternated between a CO_2 source at night and sink during the day. Although we are unaware of diurnal CO_2 flux studies in our study region, the literature suggests that such patterns likely exist, and our measurements likely overestimate the daily CO_2 uptake or underestimate the daily CO_2 efflux.

4.4 GWP of CO_2 and CH_4 emissions

Although all 32 reservoirs were a source of CH_4 to the atmosphere, eleven reservoirs had a negative combined CO_2/CH_4 GWP on a 100-year time horizon due to strong CO_2 uptake. This pattern has also been reported for small lakes in agricultural regions of the US, causing speculation that high-nutrient lakes may be net atmospheric CO_2 sinks (Balmer and Downing 2011) due to high rates of primary production. While many of the reservoirs in our study were net CO_2 sinks during daylight hours when CO_2-D was measured, it is possible that daytime uptake was offset by nighttime emissions. It is also likely that CO_2 emissions exhibit strong seasonal patterns in these temperate-zone dimictic reservoirs. For example, a study of 15 reservoirs in the Glacial Till Plains of the US found that all systems absorbed atmospheric CO_2 during the summer months, but emitted CO_2 during the remainder of the year and were net CO_2 sources at the annual scale (Jones et al. 2016). A similar seasonal pattern was previously noted for Acton Lake, an agricultural reservoir included in this study, and Burr Oak, a forested reservoir located nearby our study sites (Knoll et al. 2013). Therefore, diel and seasonal measurements are required to accurately determine the CO_2 source/sink status of temperate zone reservoirs.

Although 21 of 32 reservoirs were CO_2 sinks during the measurement period, all were sources of CH_4 and the net GWP of CO_2/CH_4 emissions was positive in 21 of the 32 sampled reservoirs for a 100-

year time horizon, indicating that these systems contribute to the radiative forcing of the atmosphere. The GWP of CO_2 emissions exceeded that of CH_4 in only 4 reservoirs, in contrast with reports from six large reservoirs in the Southeastern US where the GWP of CO_2 emissions exceeded that of CH_4, suggesting there may be important regional variation in the relative importance of these GHGs. On national and global scales, however, the GWP of CH_4 emissions from lakes and reservoirs far outweighs that of CO_2 (Li and Bush 2015, Deemer et al. 2016, DelSontro et al. 2018). Understanding the relative importance of these two gases in total reservoir GWP is important when considering mitigation strategies. For example, since CH_4 emissions are predominantly driven by ebullition, management actions that minimize the release of CH_4 rich bubbles from sediments, such as avoiding water-level drawdowns during the summer months, may mitigate CH_4 emissions (Harrison et al. 2017, Beaulieu et al. 2018), but have little effect on CO_2 emissions. Reductions in the emission of both gases should follow management actions that reduce nutrient loading to surface waters, however (Deemer et al. 2016, Beaulieu et al. 2019). Policy makers should also use the appropriate GWP horizon to weigh the relative merits of CH_4 and CO_2 emission reductions in meeting mitigation goals.

4.5 Model performance

Fifty BRTs were developed for each response variable (e.g., CH_4-T, CH_4-D) and collection of covariates (e.g., 'national', 'national + local'). Each BRT was trained and tested with unique subsets of the data and the accuracy of each model was quantified as the mean square error (MSE) of the predicted vs observed emission rates. We defined the best model as the BRT that had the lowest combined in-sample and out-of-sample MSE values, reflecting a balance between in-sample prediction accuracy and overfitting. MSE values for the best models were relatively low, even when tested against the proportion of the data not used for training the model (e.g. out-of-sample data) (Table 3). For example, the out-of-sample standardized root mean square error (osSRMSE), a measure of prediction error normalized to the mean response, ranged from 11 – 34% for CH_4-T, depending on which covariates were included in the model. Considering CH_4-T values spanned two orders of

magnitude across the study, and the well-established difficulty of predicting CH_4-T, this prediction error is quite low.

Other regional scale studies have been largely unable to identify relationships between CH_4-T and environmental drivers (Bevelhimer et al. 2016, Rinta et al. 2016), possibly because those studies used general linear modeling approaches, whereas the BRTs used in this work are better at accounting for non-linear and interactive dynamics (Elith et al. 2008). Of course, the success of any modeling approach will be partly a function of the quality of the data being modeled. A strength of the current work is that the site selection criteria (e.g., broad land use and morphology gradient) resulted in a broad range of environmental conditions while the survey design (e.g., GRTS design per waterbody) enabled accurate emission estimates. Together, these features likely enabled the pattern detection reflected in the BRT results.

Since BRTs do not have native methods for estimating model uncertainty, unlike generalized linear models, we used an empirical bootstrap (Efron 1979) to estimate the 95% confidence interval (C.I.) of the upscaled emission estimates for Ohio reservoirs. The bootstrap 95% C.I. was equivalent to 82% of the mean emission estimate, which is greater than uncertainty levels typically reported for U.S. anthropogenic CH_4 sources. For example, uncertainty in the magnitude of CH_4 emissions from enteric fermentation and landfills, the two largest anthropogenic CH_4 sources in the U.S., is equivalent to 29 and 55% of the mean, respectively (US Environmental Protection Agency 2019b). Uncertainty in the estimated magnitude of reservoir CH_4 emissions could be reduced through 1) improved identification of reservoirs in the landscape and 2) greater data availability for training predictive models.

4.6 Reservoir morphology and CH_4/CO_2 emissions

The BRTs identified descriptors of reservoir morphology as important predictors of CH_4 emission rates, with indicators of reservoir size being particularly important. For example, the models predict a negative relationship between CH_4-D and reservoir surface area (Fig. 3A, S2E), as has been previously reported for boreal lakes (Rasilo et al. 2015). Small lakes and reservoirs have several

characteristics that may promote CH_4-D including extensive littoral habitat. Methane released from littoral sediments has a short residence time in the overlying shallow water column, thereby escaping oxidation that converts a large fraction of dissolved CH_4 to CO_2 in deeper waters. This phenomenon, termed the "epilimnetic shortcut", has been demonstrated in several boreal lakes (Bastviken et al. 2008). While we did not measure CH_4 oxidation in this study, the BRTs predicted a positive relationship between littoral extent and rates of all 3 CH_4 emission mechanisms (i.e., diffusion, ebullition, total), further suggesting that littoral areas are particularly important sites for CH_4 emissions (Fig. S2G, S3H, S5F, S7E).

Maximum reservoir depth was identified as an important predictor of reservoir-scale CH_4-E, with rates falling rapidly from shallow systems to a max depth of 5-10 m, beyond which ebullition rates are predicted to remain low (Fig. 4C, S4E, S5H). This pattern is also evident at the scale of individual point measurements where ebullition was uncommon beyond depths of ~ 10m (Fig. 5). Ebullition ~ depth thresholds in the 5-10 m range have also been reported for lakes (West et al. 2016), suggesting this is a widespread pattern. The inverse relationship between ebullition rates and water depth is consistent with the well-established understanding that the total dissolved gas pressure required for bubble formation is proportional to the hydrostatic pressure at the sediment-water interface (Mattson and Likens 1990, Boudreau et al. 2005, Scandella et al. 2011), therefore more biogenic gas production is required to support bubble formation in deep versus shallow waters. While this pattern has been previously demonstrated for lakes, our work illustrates that the conceptual model also holds for reservoirs.

The BRTs identified a positive relationship between relative drainage area (RDA) and total CH_4 emission rates (Fig. 4E). Relative drainage area is the ratio of watershed-to-reservoir surface area and is positively correlated with carbon, nitrogen, and phosphorus burial rates in our study area (Knoll et al. 2014). We suggest that RDA serves as a proxy for sedimentation rates which can stimulate CH_4 production by supplying reactive organic matter to deep, anoxic sediment, thereby fueling methanogenesis (Sobek et al. 2012). Several studies have shown correlations between

sedimentation rates and CH_4 emission rates in reservoirs, including Harsha Lake, a reservoir sampled in this study (Maeck et al. 2013, de Mello et al. 2018, Berberich et al. 2019). While sedimentation rates may be important drivers of CH_4 production, the composition of watershed derived particulate matter may also play a role. The BRT also identified a positive relationship between the organic matter content of watershed soils and CH_4-T (Fig. S6A), suggesting that organic rich material eroded from the watershed stimulates methanogenesis more effectively than inorganic materials.

The BRTs also identified relationships between CO_2-T and measures of reservoir morphology. The BRT predicts greatest CO_2 uptake (i.e. a more negative CO_2 emission rate) in small reservoirs with extensive littoral zone habitat (Figs. 3G, S9F). This pattern contradicts a recent literature review indicating that CO_2 emission rates increase (i.e. become more positive) with decreasing lake size (DelSontro et al. 2018). A possible explanation for this contradiction is that TP was negatively correlated with reservoir size in this study (pearson correlation coefficient = -0.15), therefore smaller reservoirs may have had greater nutrient availability and consequently higher rates of primary productivity. This explanation is consistent with the BRT model based on local + national covariates which predicts rapidly increasing CO_2 uptake (i.e. more negative CO_2 emission rates) as a function of TP concentration (Fig. S8E). Another possibility is that littoral zone macrophytes, which can reach nuisance levels in these reservoirs (Davic et al. 1997), are a direct sink for dissolved CO_2 (Madsen and Sandjensen 1991).

4.7 Primary production and CH_4/CO_2 emissions

Several studies have shown that lentic CH_4 emission rates are correlated with system productivity, presumably because autochothony promotes hypolimnion anoxia and provides a source of labile carbon to methanogens (DelSontro et al. 2016, West et al. 2016, DelSontro et al. 2018). Our list of covariates included several indices of productivity, including estimates of watershed land-use, a proxy for nutrient loading, and in-lake measures of chla and nutrient concentrations. Surprisingly, chla did not emerge as an important predictor variable in any of the BRT models, possibly because water column chla can vary greatly on hourly and daily time scales (Rusak et al. 2018), whereas

methanogens are more tightly linked to sediment conditions which reflect productivity over longer time scales. The CH_4-D BRT showed mixed patterns in relation to productivity indices. The model predicted increasing CH_4-D with increasing agriculture on steep slopes (Fig. 4B), but an inverse relationship with TP and watershed agricultural activity (Figs. S2F, S3E). Patterns in the CH_4-T and CH_4-E BRT models were more intuitive, however, and demonstrate increasing emissions as a function of agricultural activity in the watershed (Fig. 3D, F, S4C, S5B, S5E, S6D, S6F). These patterns suggest that ebullitive and total CH_4 emissions are more closely tied to watershed condition than are diffusive emission rates, possibly because differential rates of CH_4 oxidation can obscure patterns between CH_4-D and rates of methanogenesis, whereas ebullition is largely unaffected by CH_4 oxidation (West et al. 2016).

The relationships between CO_2-T and indices of aquatic productivity were somewhat mixed. Both BRTs (i.e. national covariates only, national + local covariates) identified a general trend of increased CO_2 uptake (CO_2-T became more negative) with increasing agriculture on steep slopes, though this relationship is somewhat obscured by one observation with widespread agriculture in the watershed, but relatively low CO_2 uptake (Fig. 3H) in the national covariate model. The BRT utilizing local covariates also identified increasing CO_2 uptake with increasing TP (Fig. S8 B,E), another productivity proxy. Together, these patterns suggest that external nutrient loading, derived partly from watershed agricultural practices, stimulate aquatic primary productivity and CO_2 uptake, consistent with reports from other agricultural regions of the country (Balmer and Downing 2011). These intuitive patterns are somewhat confounded, however, by a predicted decrease in CO_2 uptake (i.e. more positive CO_2-T) with increasing agricultural in the watershed (Fig. S8D), suggesting CO_2-T responds differently to agricultural on steep versus gentle slopes, though we are unable to explain why this may be.

4.8 Local vs national predictor

We ran one set of BRTs informed with only those covariates available for all US waterbodies included in NHDPlusV2 geodatabase and a second set of BRTs which also included 'local' covariates

measured during the field survey, including measures of water chemistry and algal abundance. We expected prediction accuracy to improve when local covariates where added to the model, and for CH_4 this was the case when prediction accuracy was assessed against the training data, but not when assessed against the testing data (Table 2). Furthermore, prediction accuracy was quite good for all CH_4 models, regardless of whether local covariates were included, suggesting that CH_4 emission rates can be predicted for US reservoirs using the existing NHDPlusV2 and derivative geodatabases, without the need for additional resource intensive field-work.

Unlike the CH_4 models, prediction accuracy for the CO_2-T BRT model substantially improved when local covariates were included, due largely to the predictive power of dissolved CO_2 concentration. The BRT predicts a positive relationship between CO_2-T and dissolved CO_2 (Fig. S8A), which is consistent with well-established diffusive gas-exchange theory (MacIntyre et al. 1995). This phenomenon is also reflected in the CH_4-D BRT which identified a positive relationship between dissolved CH_4 concentration and CH_4-D, as has been previously reported for lakes in the US and Europe (Rinta et al. 2016). The model identified a negative relationship between CH_4-D and TOC (Fig. S2A), which may reflect an indirect relationship between TOC and CH_4 oxidation. Methanotrophs are inhibited by high light availability (Thottathil et al. 2018). Reduced light under high TOC conditions may therefore release methanotrophs from light inhibition, resulting in higher methanotrophic activity, lower dissolved CH_4 concentrations, and lower CH_4-D.

4.9 Limitations of modeling approach

Many of the response ~ driver relationships captured by the BRTs are consistent with established theory and previously reported results, suggesting that the models are being driven, at least in part, by fundamental ecological processes, rather than statistical artifacts such as overfitting. Like all statistical models and ML algorithms, however, BRTs may overfit training data, particularly with smaller datasets. We implemented several procedures to minimize this risk including the use of different subsets of the data to train 50 BRTs for each response ~ covariate combination, cross-validation to minimize overfitting within each training data set, a criterion specifying the minimum

number of trees in an 'acceptable' model, and a model selection criterion that gave equal weight to in-sample and out-of-sample performance. While these precautions minimize overfitting, they do not preclude it and possible evidence of overfitting can be found in partial dependence plots which do not conform to established response ~ driver relationships or are clearly driven by one or two observations. The relationship between CH_4-D and littoral extent (Fig. S3H) is an example where one or two observations seem to be driving a major feature of the partial dependence plot. Ultimately, the best way to minimize overfitting is to train the model with more data. This is not a trivial task in ecological systems where high spatial and temporal variability necessitate resource intensive sampling approaches, however. This highlights the importance of different research groups adopting comparable measurement approaches so that reports from unrelated studies can be combined for use in modeling efforts. We suggest that future studies of CH_4 emissions should include a robust statistical survey design, report system-scale emission rate estimates (+/- confidence interval) and employ measurement methods that integrate ebullition over a diurnal cycle.

4.10 Upscaling and extrapolating

We estimate that Ohio reservoirs emit 21.3 (13.3 – 30.8) Gg of CH_4 per year, which ranks as the fourth largest anthropogenic CH_4 source in the state following waste (mostly landfills), cattle enteric fermentation, and petroleum/natural gas production, processing, transmission and storage (Table 5) (US Environmental Protection Agency 2019b, a). These results reinforce previous reports that reservoirs are a significant anthropogenic CH_4 source in the US (Beaulieu et al. 2014) and suggest that future work to improve emission estimates and identify mitigation strategies is merited.

While this study was conducted at a regional scale, GHG inventory reports assembled in accordance with United Nations Framework Convention on Climate Change guidelines must be compiled at the national scale. To test the prediction accuracy of our CH_4-T BRT model at the national scale, we predicted CH_4-T for reservoirs in the US Pacific Northwest (PNW) and Southeast (SE) for which published emission rates are available (Bevelhimer et al. 2016, Harrison et al. 2017) (Fig. 6). The BRT

poorly predicted CH_4-T in these regions of the country, which isn't surprising given differences in climate, geology, and land use among the PNW, SE, and our study area. It is also possible, however, that the poor prediction accuracy partly reflects model overfitting to our observations. A national scale prediction model should be trained with data collected at the national scale. To the best of our knowledge, the only published CH_4-T rates for US reservoirs are those for 5 reservoirs in the PNW (Harrison et al. 2017), 6 in the SE (Bevelhimer et al. 2016), and 1 reservoir in Ohio from our previous work (Beaulieu et al. 2014, Beaulieu et al. 2016, Beaulieu et al. 2018). While the data presented in this study will lead to a 4-fold increase in the available literature data, there remain large portions of the US where no measurements have been made. Given that CH_4-T can vary over four orders of magnitude across reservoirs, we suggest that surveying reservoir CH_4-T at the national-scale is a critical research need that must be addressed before an unbiased estimate of US reservoir CH_4 emissions can be made. The recent adoption of IPCC reporting guidelines for GHG emissions from reservoirs underscores the importance and timeliness of this issue (Lovelock et al. 2019).

5 Conclusions

We used statistically robust survey designs and standardized methods to measure diffusive and ebullitive emissions of CO_2 and CH_4 from 32 reservoirs spanning an agriculture to forested land-use gradient, representing the largest such effort in the US. We found that all reservoirs were a source of CH_4, whereas over half were absorbing atmospheric CO_2. The GWP of combined CO_2 and CH_4 emissions on a 100-year time horizon was positive in ~70% of sampled reservoirs, with CH_4 being the more important source of GWP in most.

Our work verifies previous reports that reservoir and watershed morphology influence lentic CO_2 and CH_4 dynamics. We also found that CH_4 emission rates were positively related to indices of allochthonous carbon inputs, whereas both CH_4 and CO_2 were related to measures of watershed agricultural activity.

An important finding of our work is that the prediction accuracy of CH_4 BRT models using readily available covariate information (i.e. NHDPlusV2 and derivative databases) was roughly equivalent to

those that used information from field-based sampling efforts (i.e. water chemistry, algal abundance), suggesting that CH_4 emissions from US reservoirs can be estimated without the need for resource intensive field campaigns. This assumes that 1) models driven by national inputs will perform as well those using local inputs in other regions of the country, and 2) comparable training data are available from a nationally distributed set of reservoirs. We therefore suggest that a critical next-step in this research is to embark upon a national-scale survey of CH_4 and CO_2 emission rates from US reservoirs.

Acknowledgements

The views expressed in this paper are those of the authors and do not necessarily reflect the views or policies of the US Environmental Protection Agency. We thank the US Army Corps of Engineers, US Forest Service, Ohio Department of Natural Resources, Muskingum Watershed Conservancy District, Apple Valley Property Owners Association, RomeRock Association, Lake Mohawk Property Owners Association, and City of Akron, Ohio for site access. Field, laboratory, and GIS support was provided by Pegasus Technical Services under contract EP-C-15-010. We thank the US EPA Office of Air and Radiation for constructive discussions during this work.

Data Availability Statement

Data supporting the conclusions presented in this paper are available in the FigShare data repository (DOI: 10.6084/m9.figshare.8300531). Data and code for generating the BRTs presented in this paper are available at the reservoirGbm repository at github (http://doi.org/10.5281/zenodo.4062480).

References

Balmer, M. B., and J. A. Downing. 2011. Carbon dioxide concentrations in eutrophic lakes: undersaturation implies atmospheric uptake. Inland Waters **1**:125-132.

Barros, N., J. J. Cole, L. J. Tranvik, Y. T. Prairie, D. Bastviken, V. L. M. Huszar, P. del Giorgio, and F. Roland. 2011. Carbon emission from hydroelectric reservoirs linked to reservoir age and latitude. Nature Geoscience **4**:593-596.

Bastviken, D., J. Cole, M. Pace, and L. Tranvik. 2004. Methane emissions from lakes: Dependence of lake characteristics, two regional assessments, and a global estimate. Global Biogeochemical Cycles **18**.

Bastviken, D., J. J. Cole, M. L. Pace, and M. C. Van de Bogert. 2008. Fates of methane from different lake habitats: Connecting whole-lake budgets and CH_4 emissions. Journal of Geophysical Research-Biogeosciences **113**.

Bastviken, D., L. J. Tranvik, J. A. Downing, P. M. Crill, and A. Enrich-Prast. 2011. Freshwater Methane Emissions Offset the Continental Carbon Sink. Science **331**:50.

Beaulieu, J. J., D. A. Balz, M. K. Birchfield, J. A. Harrison, C. T. Nietch, M. C. Platz, W. C. Squier, S. Waldo, J. T. Walker, K. M. White, and J. L. Young. 2018. Effects of an Experimental Water-level Drawdown on Methane Emissions from a Eutrophic Reservoir. Ecosystems **21**:657-674.

Beaulieu, J. J., T. DelSontro, and J. A. Downing. 2019. Eutrophication will increase methane emissions from lakes and impoundments during the 21st century. Nat Commun **10**:1375.

Beaulieu, J. J., M. G. McManus, and C. T. Nietch. 2016. Estimates of reservoir methane emissions based on a spatially balanced probabilistic-survey. Limnology and Oceanography **61**:S27-S40.

Beaulieu, J. J., R. L. Smolenski, C. T. Nietch, A. Townsend-Small, and M. S. Elovitz. 2014. High Methane Emissions from a Midlatitude Reservoir Draining an Agricultural Watershed. Environmental Science & Technology **48**:11100-11108.

Berberich, M. E., J. J. Beaulieu, T. L. Hamilton, S. Waldo, and I. Buffam. 2019. Spatial variability of sediment methane production and methanogen communities within a eutrophic reservoir: Importance of organic matter source and quantity. Limnology and Oceanography.

Bergier, I., E. M. L. M. Novo, F. M. Ramos, E. A. Mazzi, and M. F. F. L. Rasera. 2011. Carbon Dioxide and Methane Fluxes in the Littoral Zone of a Tropical Savanna Reservoir (Corumbá, Brazil). Oecologia Australis **15**:666-681.

Bevelhimer, M. S., A. J. Stewart, A. M. Fortner, J. R. Phillips, and J. J. Mosher. 2016. CO2 is Dominant Greenhouse Gas Emitted from Six Hydropower Reservoirs in Southeastern United States during Peak Summer Emissions. Water **8**:14.

Bogren, K. 2001. QuikChem(R) Method 10-115-01-4-E. Total phosphorus in manual persulfate digests., Lachat Instruments, Loveland, CO, USA.

Boudreau, B. P., C. Algar, B. D. Johnson, I. Croudace, A. Reed, Y. Furukawa, K. M. Dorgan, P. A. Jumars, A. S. Grader, and B. S. Gardiner. 2005. Bubble growth and rise in soft sediments. Geology **33**:517-520.

Breiman, L., J. H. Friedman, R. A. Olshen, and C. J. Stone. 1984. Classification and Regression Trees. Wadsworth International Group, Belmont, CA, USA.

Carey, C. C., R. P. McClure, J. P. Doubek, M. E. Lofton, N. K. Ward, and D. T. Scott. 2017. Chaoborus spp. Transport CH4 from the Sediments to the Surface Waters of a Eutrophic Reservoir, But Their Contribution to Water Column CH4 Concentrations and Diffusive Efflux Is Minor. Environmental Science & Technology.

Chanton, J. P., C. S. Martens, and C. A. Kelley. 1989. Gas-transport from methane-saturated, tidal freshwater and wetland sediments. Limnology and Oceanography **34**:807-819.

Chen, Z. H., X. Q. Ye, and P. Huang. 2018. Estimating Carbon Dioxide (CO2) Emissions from Reservoirs Using Artificial Neural Networks. Water **10**.

Clow, D. W., S. M. Stackpoole, K. L. Verdin, D. E. Butman, Z. Zhu, D. P. Krabbenhoft, and R. G. Striegl. 2015. Organic Carbon Burial in Lakes and Reservoirs of the Conterminous United States. Environmental Science & Technology **49**:7614-7622.

Cole, J. J., N. F. Caraco, G. W. Kling, and T. K. Kratz. 1994. Carbon dioxide supersaturation in the surface waters of lakes. Science **265**:1568-1570.

Cole, J. J., Y. T. Prairie, N. F. Caraco, W. H. McDowell, L. J. Tranvik, R. G. Striegl, C. M. Duarte, P. Kortelainen, J. A. Downing, J. J. Middelburg, and J. Melack. 2007. Plumbing the global carbon cycle: Integrating inland waters into the terrestrial carbon budget. Ecosystems **10**:171-184.

Davic, R. D., D. Eicher, and J. DeShon. 1997. 1996 Ohio Water Resource Inventory.

de Mello, N., L. S. Brighenti, F. A. R. Barbosa, P. A. Staehr, and J. F. B. Neto. 2018. Spatial variability of methane (CH4) ebullition in a tropical hypereutrophic reservoir: silted areas as a bubble hot spot. Lake and Reservoir Management **34**:105-114.

Deemer, B. R., J. A. Harrison, S. Y. Li, J. J. Beaulieu, T. Delsontro, N. Barros, J. F. Bezerra-Neto, S. M. Powers, M. A. dos Santos, and J. A. Vonk. 2016. Greenhouse Gas Emissions from Reservoir Water Surfaces: A New Global Synthesis. Bioscience **66**:949-964.

DelSontro, T., J. J. Beaulieu, and J. A. Downing. 2018. Greenhouse gas emissions from lakes and impoundments: Upscaling in the face of global change. Limnology and Oceanography Letters **3**:64-75.

DelSontro, T., L. Boutet, A. St-Pierre, P. A. del Giorgio, and Y. T. Prairie. 2016. Methane ebullition and diffusion from northern ponds and lakes regulated by the interaction between temperature and system productivity. Limnology and Oceanography **61**:S62-S77.

DelSontro, T., M. J. Kunz, T. Kempter, A. Wuest, B. Wehrli, and D. B. Senn. 2011. Spatial Heterogeneity of Methane Ebullition in a Large Tropical Reservoir. Environmental Science & Technology **45**:9866-9873.

DelSontro, T., D. F. McGinnis, S. Sobek, I. Ostrovsky, and B. Wehrli. 2010. Extreme Methane Emissions from a Swiss Hydropower Reservoir: Contribution from Bubbling Sediments. Environmental Science & Technology **44**:2419-2425.

Demello, W. Z., and M. E. Hines. 1994. Application of static and dynamic enclosures for determining dimethyl sulfide and carbonyl sulfide exchange in *Sphagnum* peatlands: Implications for the magnitude and direction of flux. Journal of Geophysical Research-Atmospheres **99**:14601-14607.

Deshmukh, C., D. Serça, C. Delon, R. Tardif, M. Demarty, C. Jarnot, Y. Meyerfeld, V. Chanudet, P. Guédant, W. Rode, S. Descloux, and F. Guérin. 2014. Physical controls on CH4 emissions from a newly flooded subtropical freshwater hydroelectric reservoir: Nam Theun 2. Biogeosciences **11**:4251-4269.

Du, Q., H. Z. Liu, Y. Liu, L. Wang, L. J. Xu, J. H. Sun, and A. L. Xu. 2018. Factors controlling evaporation and the CO2 flux over an open water lake in southwest of China on multiple temporal scales. International Journal of Climatology **38**:4723-4739.

Efron, B. 1979. Bootstrap Methods: Another Look at the Jackknife. The Annals of Statistics **7**:1-26.

Elith, J., J. R. Leathwick, and T. Hastie. 2008. A working guide to boosted regression trees. Journal of Animal Ecology **77**:802-813.

Elzhov, T. V., K. M. Mullen, A.-N. Spiess, and B. Bolker. 2016. minpack.lm: R Interface to the Levenberg-Marquardt Nonlinear Least-Squares Algorithm Found in MINPACK, Plus Support for Bounds. R package version 1.2-1.

Erkkila, K. M., A. Ojala, D. Bastviken, T. Biermann, J. J. Heiskanen, A. Lindroth, O. Peltola, M. Rantakari, T. Vesala, and I. Mammarella. 2018. Methane and carbon dioxide fluxes over a lake: comparison between eddy covariance, floating chambers and boundary layer method. Biogeosciences **15**:429-445.

Fox, E. W., R. A. Hill, S. G. Leibowitz, A. R. Olsen, D. J. Thornbrugh, and M. H. Weber. 2017. Assessing the accuracy and stability of variable selection methods for random forest modeling in ecology. Environmental Monitoring and Assessment **189**:316.

Freeman, E. A., G. G. Moisen, J. W. Coulston, and B. T. Wilson. 2016. Random forests and stochastic gradient boosting for predicting tree canopy cover: comparing tuning processes and model performance. Canadian Journal of Forest Research **46**:323-339.

Frolking, S., N. Roulet, and J. Fuglestvedt. 2006. How northern peatlands influence the Earth's radiative budget: Sustained methane emission versus sustained carbon sequestration. Journal of Geophysical Research **111**.

Gagnon, L., C. Belanger, and Y. Uchiyama. 2002. Life-cycle assessment of electricity generation options: The status of research in year 2001. Energy Policy **30**:1267-1278.

Greenwell, B. M. 2017. pdp: An R Package for Constructing Partial Dependence Plots. R Journal **9**:421-436.

Grinham, A., M. Dunbabin, D. Gale, and J. Udy. 2011. Quantification of ebullitive and diffusive methane release to atmosphere from a water storage. Atmospheric Environment **45**:7166-7173.

Hakanson, L. 1982. Lake Bottom Dynamics and Morphometry - the Dynamic Ratio. Water Resources Research **18**:1444-1450.

Harrison, J. A., B. R. Deemer, M. K. Birchfield, and M. T. O'Malley. 2017. Reservoir Water-Level Drawdowns Accelerate and Amplify Methane Emission. Environmental Science & Technology **51**:1267-1277.

Hilgert, S., C. V. S. Fernandes, and S. Fuchs. 2019. Redistribution of methane emission hot spots under drawdown conditions. Science of the Total Environment **646**:958-971.

Hill, R. A., M. H. Weber, R. M. Debbout, S. G. Leibowitz, and A. R. Olsen. 2018. The Lake-Catchment (LakeCat) Dataset: characterizing landscape features for lake basins within the conterminous USA. Freshwater Science **37**:208-221.

Hollister, J., and J. Stachelek. 2017. lakemorpho: Calculating lake morphometry metrics in R [version 1; referees: 2 approved].

Hollister, J. W., W. B. Milstead, and M. A. Urrutia. 2011. Predicting maximum lake depth from surrounding topography. PLoS ONE **6**:e25764.

International Hydropower Association. 2010. GHG measurement guidelines for freshwater reservoirs. London.

Jammet, M., S. Dengel, E. Kettner, F. J. W. Parmentier, M. Wik, P. Crill, and T. Friborg. 2017. Year-round CH4 and CO2 flux dynamics in two contrasting freshwater ecosystems of the subarctic. Biogeosciences **14**:5189-5216.

Jones, J. R., D. V. Obrecht, J. L. Graham, M. B. Balmer, C. T. Filstrup, and J. A. Downing. 2016. Seasonal patterns in carbon dioxide in 15 mid-continent (USA) reservoirs. Inland Waters **6**:265-272.

Kalff, J. 2002. Limnology. Prentice Hall, New Jersey, USA.

Kemenes, A., B. R. Forsberg, and J. M. Melack. 2011. CO2 emissions from a tropical hydroelectric reservoir (Balbina, Brazil). Journal of Geophysical Research: Biogeosciences **116**:n/a-n/a.

Kincaid, T. M., and A. R. Olsen. 2015. spsurvey: Spatial Survey Design and Analysis. R package version 3.0.

Knoll, L. B., M. J. Vanni, W. H. Renwick, E. K. Dittman, and J. A. Gephart. 2013. Temperate reservoirs are large carbon sinks and small CO2 sources: Results from high-resolution carbon budgets. Global Biogeochemical Cycles **27**:52-64.

Knoll, L. B., M. J. Vanni, W. H. Renwick, and S. Kollie. 2014. Burial rates and stoichiometry of sedimentary carbon, nitrogen and phosphorus in Midwestern US reservoirs. Freshwater Biology **59**:2342-2353.

Koschorreck, M., I. Hentschel, and B. Boehrer. 2017. Oxygen Ebullition From Lakes. Geophysical Research Letters **44**:9372-9378.

Lapierre, J.-F., D. A. Seekell, C. T. Filstrup, S. M. Collins, C. Emi Fergus, P. A. Soranno, and K. S. Cheruvelil. 2017. Continental-scale variation in controls of summer CO2 in United States lakes. Journal of Geophysical Research: Biogeosciences **122**:875-885.

Lazzarino, J. K., R. W. Bachmann, M. V. Hoyer, and D. E. Canfield. 2009. Carbon dioxide supersaturation in Florida lakes. Hydrobiologia **627**:169-180.

Li, S., and R. T. Bush. 2015. Revision of methane and carbon dioxide emissions from inland waters in India. Global Change Biology **21**:6-8.

Liden, R. 2013. Interim Technical Note: Greenhouse gases from reservoirs caused by biochemical processes. World Bank.

Liu, H. P., Q. Y. Zhang, G. G. Katul, J. J. Cole, F. S. Chapin, and S. MacIntyre. 2016. Large CO_2 effluxes at night and during synoptic weather events significantly contribute to CO_2 emissions from a reservoir. Environmental Research Letters **11**.

Lovelock, C. E., C. Evans, N. Barros, Y. T. Prairie, J. Alm, D. Bastviken, J. J. Beaulieu, M. Garneau, A. Harby, J. A. Harrison, D. Pare, H. L. Raadal, B. Sherman, C. Zhang, and S. M. Ogle. 2019. Chapter 7-Wetlands. 2019 Refinement to the 2006 Guidelines for National Greenhouse Gas Inventories.

MacIntyre, S., R. Wanninkhof, and J. P. Chanton. 1995. Trace gas exchange across the air-water interface in freshwater and coastal marine environments. Pages 52-97 *in* P. A. Matson and R. C. Harriss, editors. Biogenic trace gases: measuring emissions from soil and water. Blackwell Science, London.

Madsen, T. V., and K. Sandjensen. 1991. Photosynthetic Carbon Assimilation in Aquatic Macrophytes. Aquatic Botany **41**:5-40.

Maeck, A., T. DelSontro, D. F. McGinnis, H. Fischer, S. Flury, M. Schmidt, P. Fietzek, and A. Lorke. 2013. Sediment trapping by dams creates methane emission hot spots. Environmental Science & Technology **47**:8130-8137.

Maher, D. T., M. Drexl, D. R. Tait, S. G. Johnston, and L. C. Jeffrey. 2019. iAMES: An inexpensive, Automated Methane Ebullition Sensor. Environmental Science & Technology **53**:6420-6426.

Mattson, M. D., and G. E. Likens. 1990. Air pressure and methane fluxes. Nature **347**:718-719.

McGinnis, D. F., J. Greinert, Y. Artemov, S. E. Beaubien, and A. Wüest. 2006. Fate of rising methane bubbles in stratified waters: How much methane reaches the atmosphere? Journal of Geophysical Research **111**:C09007.

McKay, L., T. Bondelid, T. Dewald, J. Johnson, R. Moore, and A. Rea. 2018. NHDPlus Version 2: User Guide (Data Model Version 2.1).

Mosher, J. J., A. M. Fortner, J. R. Phillips, M. S. Bevelhimer, A. J. Stewart, and M. J. Troia. 2015. Spatial and Temporal Correlates of Greenhouse Gas Diffusion from a Hydropower Reservoir in the Southern United States. Water **7**:5910-5927.

Musenze, R. S., A. Grinham, U. Werner, D. Gale, K. Sturm, J. Udy, and Z. Yuan. 2014. Assessing the spatial and temporal variability of diffusive methane and nitrous oxide emissions from subtropical freshwater reservoirs. Environmental Science & Technology **48**:14499-14507.

Nakagawa, F., N. Yoshida, Y. Nojiri, and V. N. Makarov. 2002. Production of methane from alassesin eastern Siberia: Implications from its C-14 and stable isotopic compositions. Global Biogeochemical Cycles **16**.

Natchimuthu, S., B. P. Selvam, and D. Bastviken. 2014. Influence of weather variables on methane and carbon dioxide flux from a shallow pond. Biogeochemistry **119**:403-413.

Natchimuthu, S., I. Sundgren, M. Galfalk, L. Klemedtsson, P. Crill, A. Danielsson, and D. Bastviken. 2016. Spatio-temporal variability of lake CH4 fluxes and its influence on annual whole lake emission estimates. Limnology and Oceanography **61**:S13-S26.

Olsen, A. R., T. M. Kincaid, and Q. Payton. 2012. Spatially balanced survey designs for natural resources. Pages 126-150 *in* R. A. Gitzen, J. J. Millspaugh, A. B. Cooper, and D. S. Licht, editors. Design and analysis of long-term ecological monitoring studies. Cambridge University Press, United Kingdom.

Papale, D., and A. Valentini. 2003. A new assessment of European forests carbon exchanges by eddy fluxes and artificial neural network spatialization. Global Change Biology **9**:525-535.

Podgrajsek, E., E. Sahlee, and A. Rutgersson. 2014. Diurnal cycle of lake methane flux. Journal of Geophysical Research-Biogeosciences **119**:236-248.

Prairie, Y. T., J. Alm, J. Beaulieu, N. Barros, T. Battin, J. Cole, P. del Giorgio, T. DelSontro, F. Guérin, A. Harby, J. Harrison, S. Mercier-Blais, D. Serça, S. Sobek, and D. Vachon. 2017a. Greenhouse Gas Emissions from Freshwater Reservoirs: What Does the Atmosphere See? Ecosystems.

Prairie, Y. T., J. Alm, A. Harby, and S. Mercier-Blais. 2017b. The GHG Reservoir Tool (G-res) User guide. UNESCO/IHA research project on the GHG status of freshwater reservoirs.

R Development Core Team. 2016. R: A Language and Environment for Statistical Computing. R Foundation for Statistical Computing, Vienna, Austria.

Rasilo, T., Y. T. Prairie, and P. A. Del Giorgio. 2015. Large-scale patterns in summer diffusive CH4 fluxes across boreal lakes, and contribution to diffusive C emissions. Global Change Biology **21**:1124-1139.

Reis, P. C., and F. A. Barbosa. 2014. Diurnal sampling reveals significant variation in CO2 emission from a tropical productive lake. Brazilian Journal of Biology **74**:S113-119.

Ridgeway, G. 2017. gbm: Generalized boosted regression models. R package version 2.1.3.

Rinta, P., D. Bastviken, J. Schilder, M. Van Hardenbroek, T. Stötter, and O. Heiri. 2016. Higher late summer methane emission from central than northern European lakes. Journal of limnology **76**.

Rudd, J. W. M., R. Harris, C. A. Kelly, and R. E. Hecky. 1993. Are Hydroelectric Reservoirs Significant Sources of Greenhouse Gases. Ambio **22**:246-248.

Rusak, J. A., A. J. Tanentzap, J. L. Klug, K. C. Rose, S. P. Hendricks, E. Jennings, A. Laas, D. Pierson, E. Ryder, R. L. Smyth, D. S. White, L. A. Winslow, R. Adrian, L. Arvola, E. de Eyto, H. Feuchtmayr, M. Honti, V. Istvánovics, I. D. Jones, C. G. McBride, S. R. Schmidt, D. Seekell, P. A. Staehr, and

G. Zhu. 2018. Wind and trophic status explain within and among-lake variability of algal biomass. **3**:409-418.

Scandella, B. P., C. Varadharajan, H. F. Hemond, C. Ruppel, and R. Juanes. 2011. A conduit dilation model of methane venting from lake sediments. Geophysical Research Letters **38**.

Schapire, R. 2003. The boosting approach to machine learning - an overview.*in* D. D. Denison, M. H. Hansen, C. Holmes, B. Mallick, and B. Yu, editors. MSRI workshop on nonlinear estimation and classification, 2002. Springer, New York, USA.

Smith, P., and K. Bogren. 2003. QuickChem Method 10-107-04-4-A. Determination of nitrate/nitrite in manual persulfate digestions., Lachat Instruments, Loveland, CO.

Sobek, S., G. Algesten, A.-K. Bergstrom, M. Jansson, and L. J. Tranvik. 2003. The catchment and climate regulation of pCO2 in boreal lakes. Global Change Biology **9**:630-641.

Sobek, S., T. DelSontro, N. Wongfun, and B. Wehrli. 2012. Extreme organic carbon burial fuels intense methane bubbling in a temperate reservoir. Geophysical Research Letters **39**:L01401.

Soumis, N., E. Duchemin, R. Canuel, and M. Lucotte. 2004. Greenhouse gas emissions from reservoirs of the western United States. Global Biogeochemical Cycles **18**.

Spafford, L., and D. Risk. 2018. Spatiotemporal Variability in Lake-Atmosphere Net CO2 Exchange in the Littoral Zone of an Oligotrophic Lake. Journal of Geophysical Research: Biogeosciences **123**:1260-1276.

St. Louis, V. L., C. A. Kelly, É. Duchemin, J. W. M. Rudd, and D. M. Rosenberg. 2000. Reservoir surfaces as sources of greenhouse gases to the atmosphere: A global estimate. Bioscience **50**:766-775.

Stevens, D. L., and A. R. Olsen. 2003. Variance estimation for spatially balanced samples of environmental resources. Environmetrics **14**:593-610.

Stocker, T. F., D. Qin, G.-K. Plattner, M. M. B. Tignor, S. K. Allen, J. Boschung, A. Nauels, Y. Xia, V. Bex, and P. M. Midgley, editors. 2013. Climate Change 2013: The Physical Science Basis. Cambridge University Press, New York, NY.

Stolk, P. C., C. M. J. Jacobs, E. J. Moors, A. Hensen, G. L. Velthof, and P. Kabat. 2009. Significant non-linearity in nitrous oxide chamber data and its effect on calculated annual emissions. Biogeosciences Discuss. **6**:115-141.

Sturm, K., Z. Yuan, B. Gibbes, U. Werner, and A. Grinham. 2014. Methane and nitrous oxide sources and emissions in a subtropical freshwater reservoir, South East Queensland, Australia. Biogeosciences **11**:5245-5258.

Thottathil, S., P. C. J. Reis, P. Del Giorgio, and Y. T. Prairie. 2018. The Extent and Regulation of Summer Methane Oxidation in Northern Lakes. Journal of Geophysical Research: Biogeosciences.

Tranvik, L. J., J. A. Downing, J. B. Cotner, S. A. Loiselle, R. G. Striegl, T. J. Ballatore, P. Dillon, K. Finlay, K. Fortino, L. B. Knoll, P. L. Kortelainen, T. Kutser, S. Larsen, I. Laurion, D. M. Leech, S. L. McCallister, D. M. McKnight, J. M. Melack, E. Overholt, J. A. Porter, Y. Prairie, W. H. Renwick, F. Roland, B. S. Sherman, D. W. Schindler, S. Sobek, A. Tremblay, M. J. Vanni, A. M. Verschoor, E. von Wachenfeldt, and G. A. Weyhenmeyer. 2009. Lakes and reservoirs as regulators of carbon cycling and climate. Limnology and Oceanography **54**:2298-2314.

U.S. Geological Survey. 2014. NLCD 2011 Land Cover (2011 Edition, amended 2014) - National Geospatial Data Asset (NGDA) Land Use Land Cover *in* U. S. G. Survey, editor. U.S. Geological Survey, Sioux Falls, SD.

United States Army Corps of Engineers. 2013. National Inventory of Dams.

US Environmental Protection Agency. 2019a. Greenhouse gas emissions from large facilities.

US Environmental Protection Agency. 2019b. Inventory of U.S. Greenhouse Gas Emissions and Sinks: 1990-2017. EPA 430-R-19-001.

Varadharajan, C., and H. F. Hemond. 2012. Time-series analysis of high-resolution ebullition fluxes from a stratified, freshwater lake. Journal of Geophysical Research-Biogeosciences **117**.

Vesala, T., J. Huotari, U. Rannik, T. Suni, S. Smolander, A. Sogachev, S. Launiainen, and A. Ojala. 2006. Eddy covariance measurements of carbon exchange and latent and sensible heat fluxes over a boreal lake for a full open-water period. Journal of Geophysical Research-Atmospheres **111**.

Walter, K. M., J. P. Chanton, F. S. Chapin, E. A. G. Schuur, and S. A. Zimov. 2008. Methane production and bubble emissions from arctic lakes: Isotopic implications for source pathways and ages. Journal of Geophysical Research-Biogeosciences **113**.

West, W. E., K. P. Creamer, and S. E. Jones. 2016. Productivity and depth regulate lake contributions to atmospheric methane. Limnology and Oceanography **61**:S51-S61.

Wik, M., B. F. Thornton, D. Bastviken, J. Uhlbäck, and P. M. Crill. 2016. Biased sampling of methane release from northern lakes: A problem for extrapolation. Geophysical Research Letters **43**:1256-1262.

Winslow, L. A., J. S. Read, P. C. Hanson, and E. H. Stanley. 2014. Lake shoreline in the contiguous United States: quantity, distribution and sensitivity to observation resolution. Freshwater Biology **59**:213-223.

Xu, Y. J., Z. Xu, and R. Yang. 2019. Rapid daily change in surface water pCO2 and CO2 evasion: A case study in a subtropical eutrophic lake in Southern USA. Journal of Hydrology **570**:486-494.

Zhao, Y., B. Sherman, P. Ford, M. Demarty, T. DelSontro, A. Harby, A. Tremblay, I. B. Overjordet, X. F. Zhao, B. H. Hansen, and B. F. Wu. 2015. A comparison of methods for the measurement of CO2 and CH4 emissions from surface water reservoirs: Results from an international workshop held at Three Gorges Dam, June 2012. Limnology and Oceanography-Methods **13**:15-29.

Table 1. Predictor variables used in boosted regression trees to model methane and carbon dioxide emission rates.

Variable	Units	Mean	Range
Local variables			
chl a	µg L^{-1}	17.2	1.5 – 61.4
TP	µg L^{-1}	84.3	7.9 – 772.7
TN	µg L^{-1}	1202.9	231.4 – 3463.0
TOC	mg L^{-1}	5.3	2.5 – 15.4
*dissolved CH_4	µmol L^{-1}	3.58	0.43 – 18.55
*dissolved CO_2	µmol L^{-1}	121.4	26.0 – 244.9
proportion hypoxic	--	0.11	0 – 0.69
proportion hypolimnetic	--	0.22	0 – 0.73
National variables			
max depth	m	13.3	2.7 – 35.1
depth ratio	--	0.39	0.16 – 1.13
dynamic ratio	--	0.57	0.12 – 1.80
proportion < 3m deep	--	0.42	0.01 – 1.0
†reservoir area	km^2	6.27	1.04 – 32.2
relative drainage area	--	82.7	5.7 – 385.9
percent agriculture	%	43.5	0.1 – 83.9
percent agriculture on slopes > 10%	%	34	0 – 17.3
surface soil erodibility factor	--	0.38	0.31 – 0.43
soil organic matter	% by weight	0.97	0.31 – 6.20
runoff	mm	405	325 – 520
30-year normal mean air temperature	C^o	10.6	9.3 – 12.7

*Units of mol L^{-1} were used in boosted regression tree models. †Units of m^2 were used in boosted regression tree models.

Table 2. Total methane emission rates (mean (95% C.I.)) measured during four surveys conducted at Acton Lake.

Sample Dates	CH_4-T (mg m^{-2} h^{-1})
2016-05-31	5.1 (3.6 – 6.6)
2017-07-10	8.2 (5.1 – 11.3)
2017-08-31	11.2 (7.5 – 14.9)
2017-10-04	12.3 (8.7 – 16.0)
Overall mean	9.2 (6.2 – 12.2)

Table 3. Standardized root mean square error (SRMSE) of boosted regression tree predictions against training and testing data for diffusive, ebullitive and total CH4 emission rates and total CO2 emission rates. Coefficient of determination (R^2) of model predictions is reported for testing data. 'national' covariates are predictor variables available from the National Hydrography Dataset (NHDPlusV2) and related data products. 'national + local' covariates include NHD variables and additional measurements made on-site during the field survey (i.e. nutrient chemistry)

			training			testing	
Response variable	Covariates	Optimal trees	isMSE	isSRMSE	R^2	osMSE	osSRMSE
diffusive CH_4	national	12803	0.38	0.40	0.87	0.41	0.42
	national + local	19976	0.17	0.26	0.90	0.54	0.46
ebullitive CH_4	national	19987	1.72	0.24	0.98	2.28	0.28
	national + local	16760	0.52	0.13	0.99	3.42	0.33
total CH_4	national	19984	0.91	0.15	0.99	0.46	0.11
	national + local	17190	0.56	0.11	0.99	5.55	0.34
total CO_2	national	14813	1565	-4.29	0.73	734	-2.94
	national + local	8935	730	-1.65	0.91	274	-1.01

Table 4. List of covariates leading to an average of at least a 5% reduction in mean square error when excluded from the model. These represent the most important variables in each boosted regression trees are listed in order of decreasing importance for each model.

Response variable	Covariates	Variable	Relative Influence
CH_4-D	National and local covariates	TOC	15.7
		ag on slope > 10%	14.6
		dissolved CH_4	14.6
		reservoir area	12.8
		TP	12.4
		proportion <3m deep	5.9
		soil organic matter	5.1
CH_4-D	National covariates	reservoir area	23.0
		ag on slope > 10%	14.3
		soil organic matter	10.1
		percent ag	9.4
		dynamic ratio	8.4
		relative drainage area	6.6
		depth ratio	5.9
		proportion <3m deep	5.6
CH_4-E	National and local covariates	relative drainage area	25.2
		proportion hypolimnetic	17.4
		percent ag	13.1
		dissolved CO_2	9.3
		max depth	9.1
		proportion hypoxic	6.2
CH_4-E	National covariates	relative drainage area	21.4
		percent ag	15.3
		dynamic ratio	10.3
		soil erodibility factor	9.4
		ag on slope > 10%	7.7
		proportion <3m deep	7.4
		depth ratio	7.1
		max depth	6.6
		mean air temperature	6.3
CH_4-T	National and local covariates	soil organic matter	29.7
		depth ratio	11.8
		relative drainage area	10.1
		percent ag	8.0
		dissolved CO_2	7.3
		ag on slope > 10%	6.9
		proportion hypolimnetic	5.7
CH_4-T	National covariates	relative drainage area	21.6
		depth ratio	20.0
		max depth	16.6
		percent ag	11.6
		proportion < 3m deep	7.0
		runoff	5.1
CO_2-T	National and local covariates	dissolved CO_2	47.4
		ag on slope > 10%	14.5
		proportion hypoxic	6.9
		percent ag	6.1
		TP	5.8
CO_2-T	National covariates	depth ratio	23.8
		proportion < 3m deep	19.2
		runoff	15.8
		relative drainage area	9.2
		ag on slope > 10%	7.8
		reservoir area	6.9
		soil erodibility factor	5.0

Table 5. Anthropogenic methane sources in Ohio. Reservoir emissions were estimate with this work and all other sources are for the year 2017. Enteric fermentation was taken from the Inventory of U.S. Greenhous Gas Emissions and Sinks: 1990-2017 (Table A-182;US Environmental Protection Agency 2019b). All other sources were taken from the U.S. EPA's Greenhouse Gas Emissions from Large Facilities program (US Environmental Protection Agency 2019b).

Sector	CH_4 emission ($Gg\ CH_4\ y^{-1}$)
waste	187.0
enteric fermentation	93.4
petroleum and natural gas	29.6
reservoir	21.3
underground coal mines	14.3
power plants	6.4
refineries	0.8
ponds	0.3 – 1.5
metals	0.3

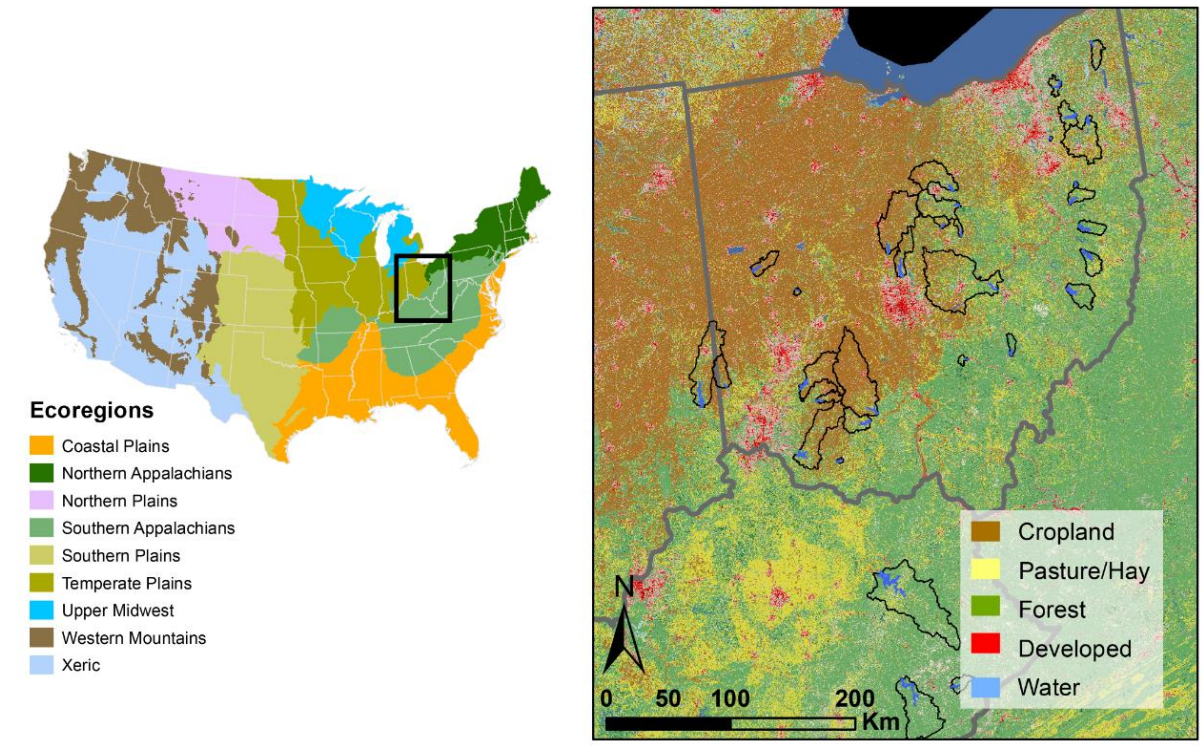

Figure 1. Site map illustrating major US ecoregions and location of 32 sampled reservoirs in study area. Reservoir surface area is shown in blue and watershed boundaries are delineated in black.

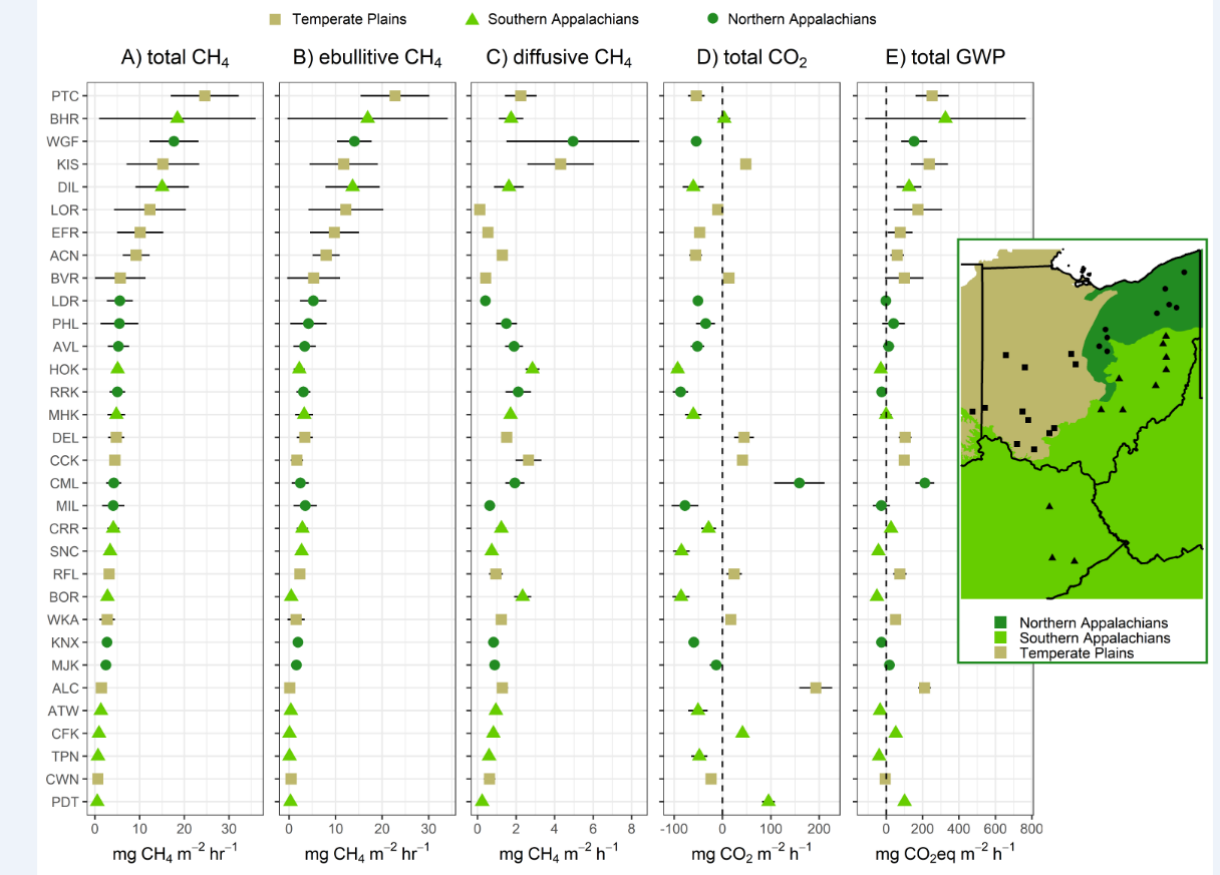

Figure 2. Reservoir scale mean emission rates and 95% confidence interval for A) total CH_4 emissions, B) ebullitive CH_4 emissions, C) diffusive CH_4 emissions, D) total CO_2 emissions, and E) global warming potential (GWP). Vertical dashed line in panels D and E indicate emission rates of 0. Inset map shows location of study sites relative to the states of Ohio, Kentucky, Indiana, and the three major ecoregions in the study area.

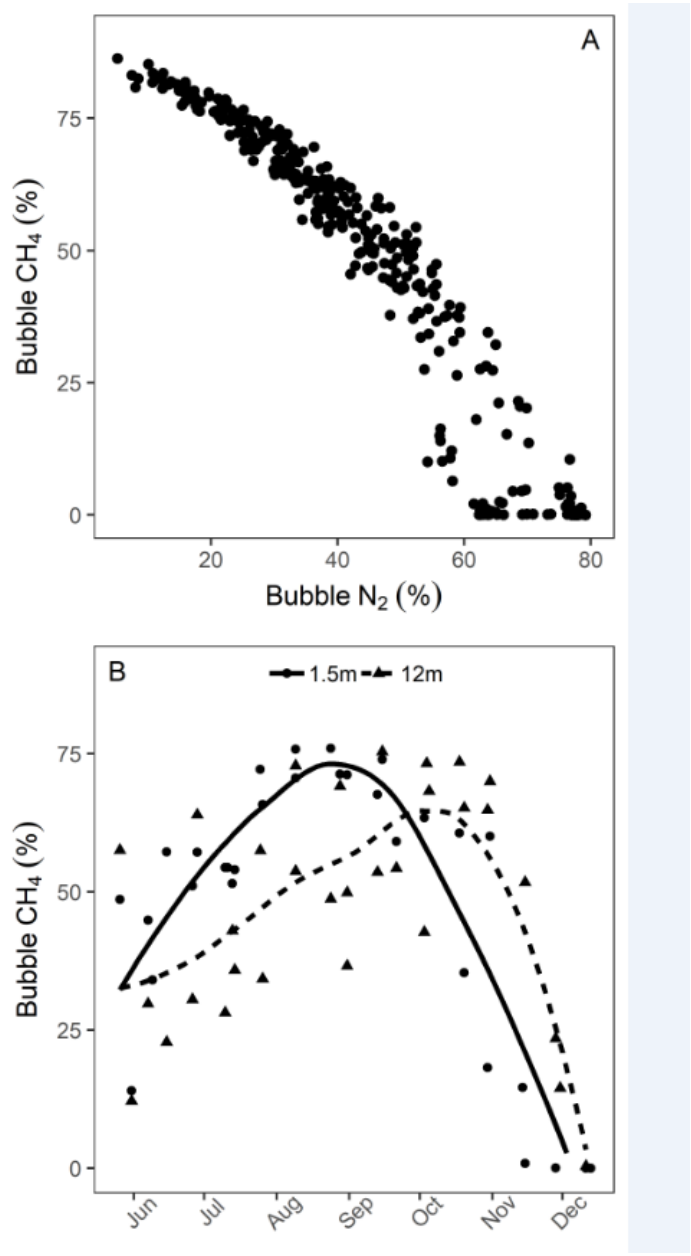

Figure 3. A) CH_4 and N_2 content of bubbles collected during the 2016 survey. B) Bubble CH_4 content during two years (2017-2018) of biweekly sampling at a deep (12m) and shallow (1.5m) site at Acton Lake. Solid and dashed lines represent LOESS smoothers.

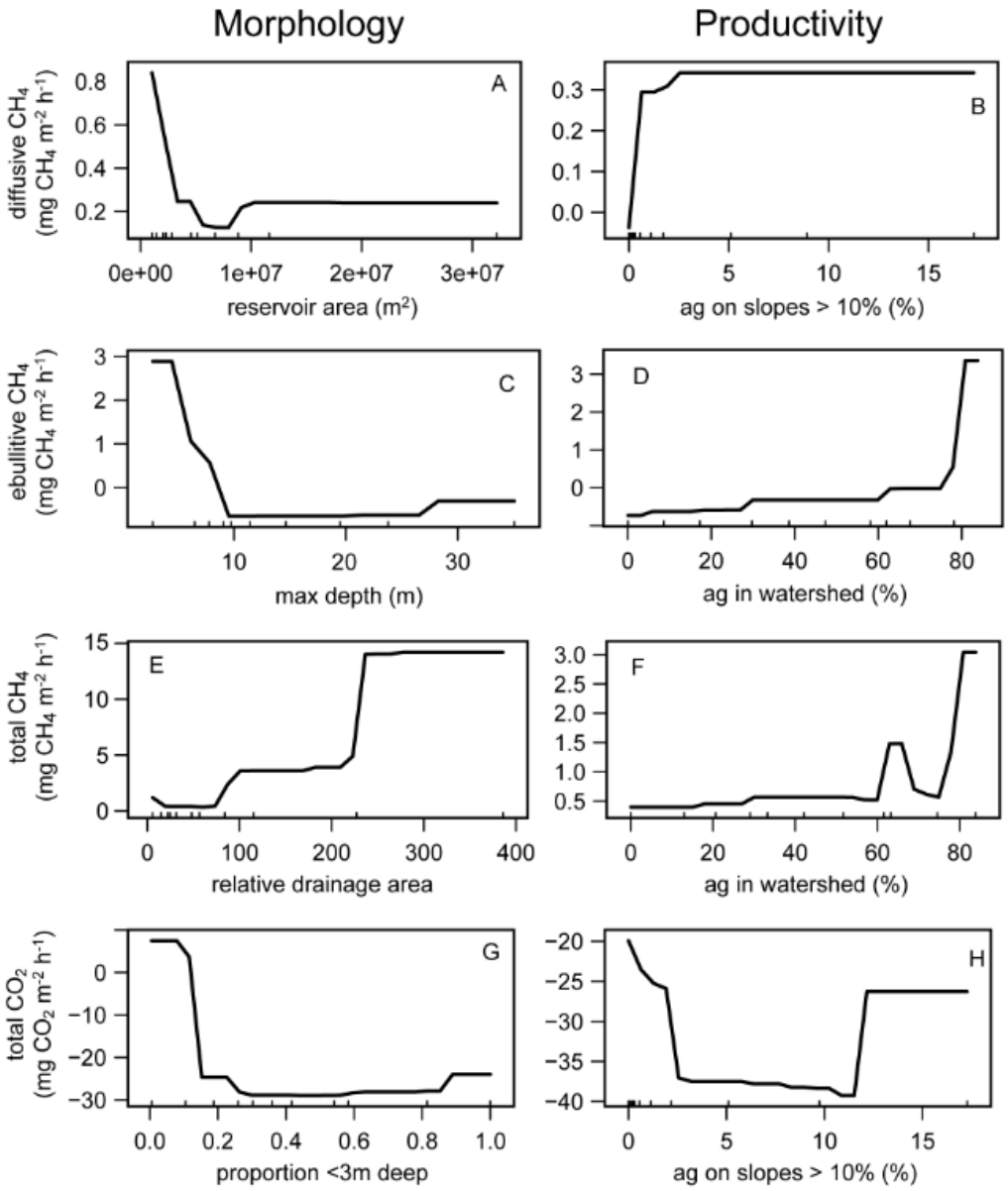

Figure 4. Partial dependence plots for boosted regression trees using only national covariates for A-B) diffusive CH_4 emission rates, C-D) ebullitive CH_4 emission rates, E-F) total CH_4 emission rates, and G-H) total CO_2 emission rates. Vertical ticks along x-axis represent observations included in the training data.

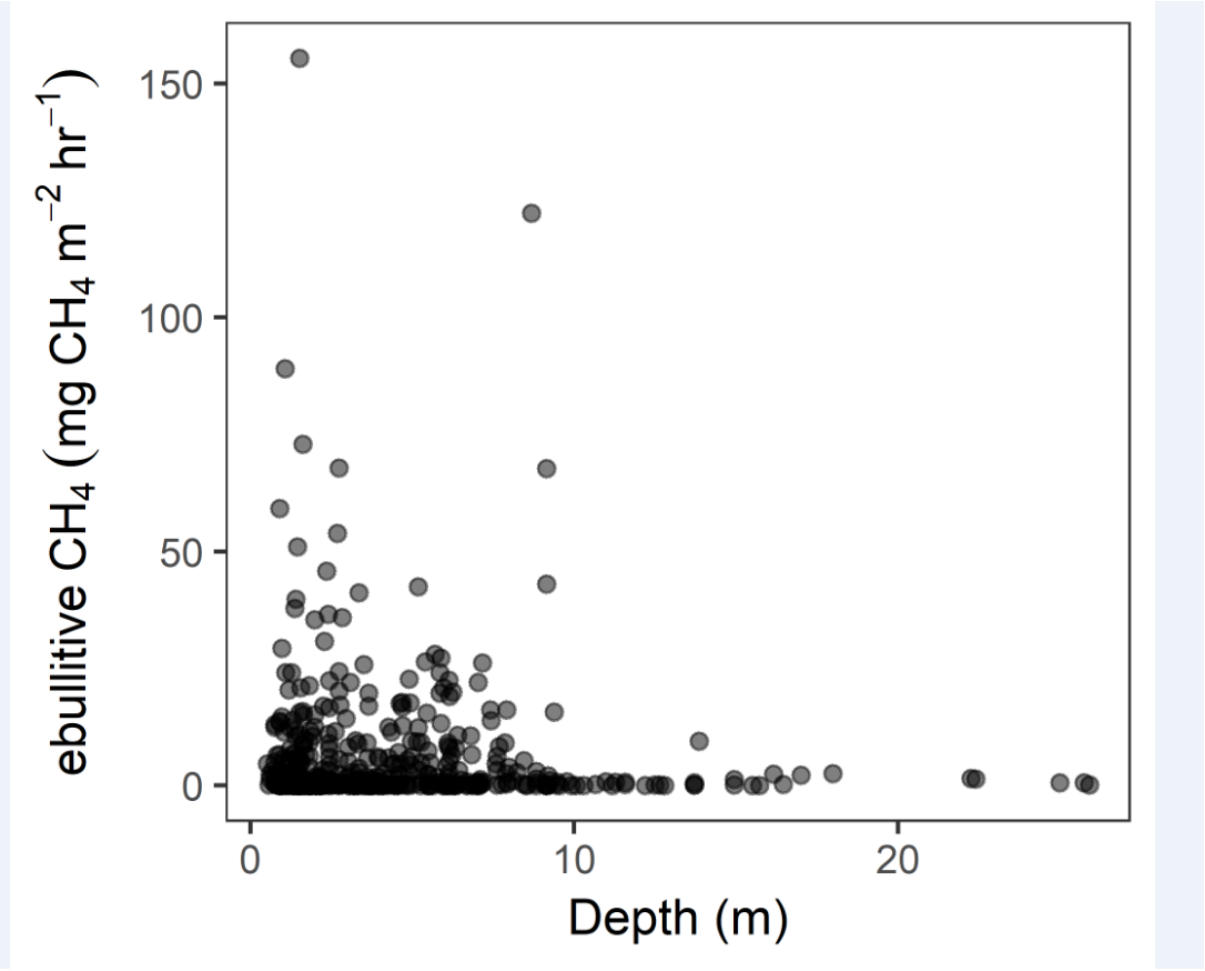

Figure 5. Ebullitive CH_4 emission rate versus water depth for 536 point measurements across the 32 reservoirs in this study. Symbol shading reflects the number of observations at any x, y coordinate. Dark and light shading reflect a high and low density of observations, respectively.

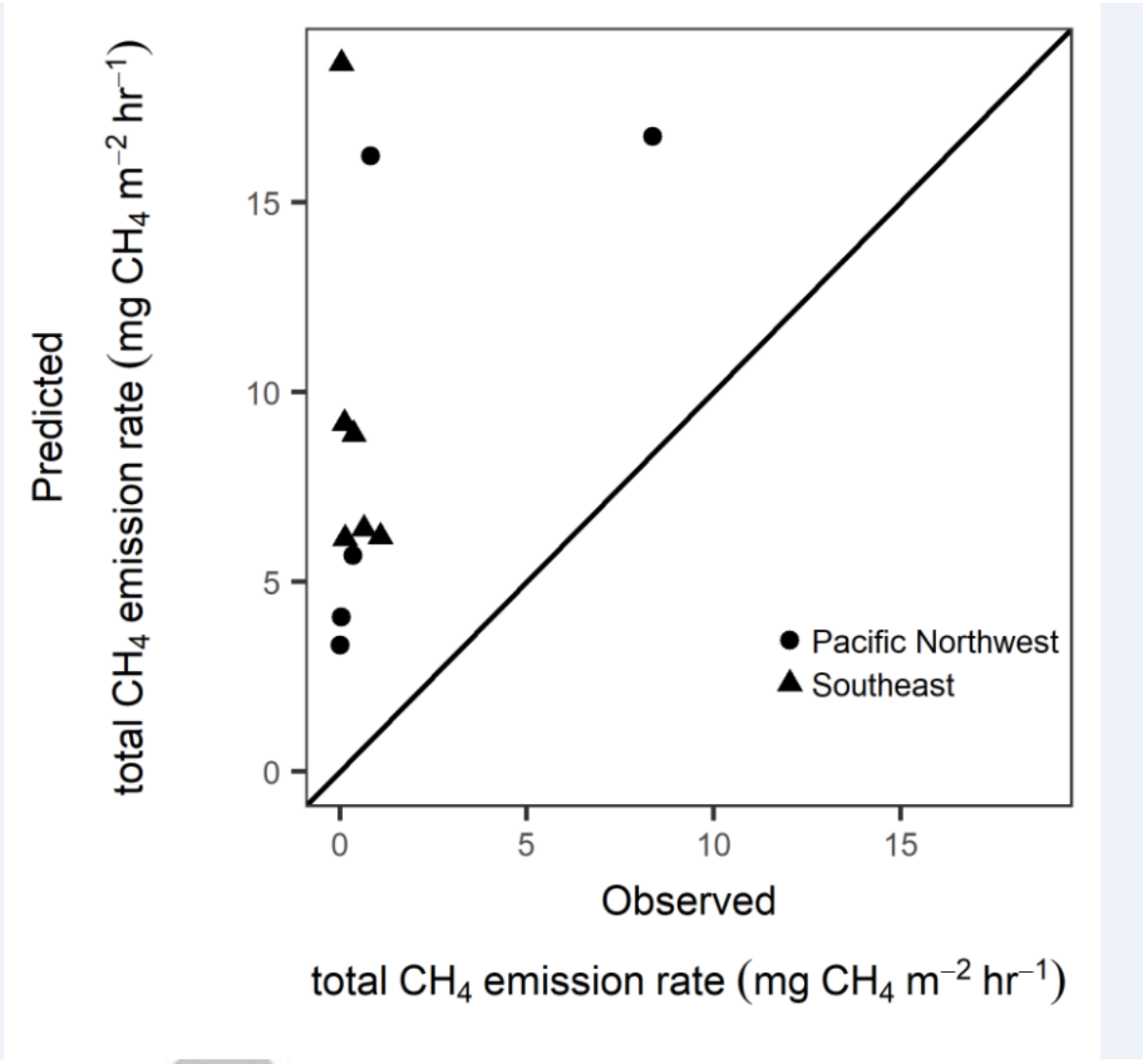

Figure 6. Predicted vs observed CH_4-T for reservoirs in the U.S. Pacific Northwest and Southeast. Predictions were made using the BRT trained on field data collected in Ohio, Kentucky, and Indiana during this study.